Arbitrary dimensional Majorana dualities and architectures for topological matter

Zohar Nussinov,[1] Gerardo Ortiz,[2] and Emilio Cobanera[2]

[1]*Department of Physics, Washington University, St. Louis, Missouri 63160, USA*
[2]*Department of Physics, Indiana University, Bloomington, Indiana 47405, USA*

Motivated by the prospect of attaining Majorana modes at the ends of nanowires, we analyze *interacting* Majorana systems on general networks and lattices in an arbitrary number of dimensions, and derive universal spin duals. We prove that these interacting Majorana systems, quantum Ising gauge theories, and transverse-field Ising models with annealed bimodal disorder are all dual to one another on general planar graphs. This leads to an interesting connection between heavily disordered annealed Ising systems and uniform Ising theories with nearest-neighbor interactions. As any Dirac fermion (including electronic) operator can be expressed as a linear combination of two Majorana fermion operators, our results further lead to dualities between interacting Dirac fermionic systems on rather general lattices and graphs and corresponding spin systems. Such general complex Majorana architectures (other than those of simple square or other crystalline arrangements) might be of empirical relevance. As these systems display low-dimensional symmetries, they are candidates for realizing topological quantum order. The spin duals allow us to predict the feasibility of various standard transitions as well as spin-glass-type behavior in *interacting* Majorana fermion or electronic systems. Several systems that can be simulated by arrays of Majorana wires are further introduced and investigated: (1) the *XXZ honeycomb compass* model (intermediate between the classical Ising model on the honeycomb lattice and Kitaev's honeycomb model), (2) a checkerboard lattice realization of the model of Xu and Moore for superconducting ($p + ip$) arrays, and a (3) compass-type two-flavor Hubbard model with both pairing and hopping terms. By the use of our dualities (tantamount to high-dimensional fermionization), we show that all of these systems lie in the three-dimensional Ising universality class. We further discuss how the existence of topological orders and bounds on autocorrelation times can be inferred by the use of symmetries and also propose to engineer *quantum simulators* via such Majorana wire networks.

I. INTRODUCTION

Majorana (contrary to Dirac) fermions are particles that constitute their own antiparticles.[1] Early quests for Majorana fermions centered on neutrinos and fundamental issues in particle physics that have yet to be fully settled. If neutrinos were Majorana fermions, then neutrinoless double-β decay would be possible and thus experimentally observed. More recently, there has been a flurry of activity in the study of Majorana fermions in candidate condensed matter realizations,[2–17] including lattice[18–20] and other[8,9] systems inspired by the prospect of topological quantum computing.[21,22] In the condensed matter arena, Majorana fermions are, of course, not fundamental particles, but rather emerge as collective excitations of the basic electronic constituents. The systems discussed in this work form a generalization of a model[20] that largely builds and expands on ideas considered by Kitaev[8,18,21] including, notably, the feasibility of creating Majorana fermions at the endpoints of nanowires.[23] A quadratic fermionic Hamiltonian for electronic hopping along a wire in the presence of superconducting pairing terms (induced by a proximity effect to bulk superconducting grains on which the wire is placed) can be expressed as a Majorana fermion bilinear that may admit free unpaired Majorana fermion modes at the wire endpoints.[23] Kitaev's proposal entailed *p*-wave superconductors.[8]

More recent and detailed studies suggest simpler and more concrete ways in which zero-energy Majorana modes might explicitly appear at the endpoints of nanowires placed close to (conventional *s*-wave) superconductors. Some of the best-known proposals[7,9,11] entail semiconductor nanowires [e.g., InAs or InSb (Ref. 24)] with strong depolarizing Rashba spin-orbit coupling that are immersed in a magnetic field that leads to a competing Zeeman effect. These wires are to be placed close to superconductors in order to trigger superconducting pairing terms in the wire. By employing the Bogoliubov–de Gennes equation to study the band structure, it was readily seen how Majorana modes appear when the band gap vanishes.[7,9,11] Along another route, it was predicted that zero-energy Majorana fermions might appear at an interface between a superconductor and a ferromagnet.[6,19] Majorana modes may also appear in time-reversal-invariant *s*-wave topological superconductors.[16]

If zero-energy Majorana fermions may indeed be *harvested* in these or other ways,[7] then it will be natural to consider what transpires in general networks made of such nanowires. The possible rich architecture of structures constructed out of Majorana wires and/or particular junctions may allow for interesting collective phenomena as well as long sought topological quantum computing applications.[21,22] Interestingly, as is well appreciated, the braiding of (degenerate) Majorana fermions realizes a non-Abelian unitary transformation that may prove useful in quantum computing, providing further impetus to this problem. In this work, we consider general questions related to Majorana fermion systems that may be constructed from nanowire architectures. In order to understand many of these and other systems, it is necessary to study *interacting* Majorana fermion systems. To facilitate this goal, we will introduce and employ dualities between interacting Majorana fermion theories and earlier heavily studied spin systems.

A. Summary of results

A principal aim of this article is to derive dualities between interacting Majorana fermion systems and Pauli ($S = 1/2$) spin models and to explore consequences of these dualities. As many $S = 1/2$ spin models have been heavily investigated throughout the years, the dualities that we will report on will allow a valuable tool for, nearly immediately, obtaining numerous hitherto unknown results for a multitude of interacting Majorana fermion systems. Toward this end, we will invoke a general framework for dualities that does not require the incorporation of known explicit representations of a spin in terms of Majorana fermions nor Jordan-Wigner transformations that have been invoked in earlier works.[19,20,25] The bond-algebraic approach[26–32] that we employ to study general *exact* dualities and fermionization[30,31] allows for the derivation of earlier known dualities as well as a plethora of many new others for rather general networks (or planar graphs) in arbitrary dimensions and boundary conditions. (In the following general or arbitrary networks refer to planar graphs.) It is important to note, as we will return to explicitly later, that as Dirac fermions can be expressed as a linear combination of two Majorana fermions, our mappings lead to dualities between standard (non-Majorana) fermionic systems and spin systems on arbitrary graphs in general dimensions. These afford non-trivial examples of fermionization in more than one dimension.

Among several exact dualities that we introduce here, we note, in particular, the following:

(i) A duality, in arbitrary dimension, between the Majorana fermion system corresponding to an arbitrary network of nanowires on superconducting grains and quantum Ising gauge (QIG) theories.

(ii) Gauge-reducing emergent dualities,[31] in arbitrary number of dimensions, between granular Majorana fermion systems on an arbitrary network and transverse-field Ising models with annealed exchange couplings. In two dimensions, this duality, along with the first one listed above, indicates that an annealed average over a random exchange may leave the system identical to a uniform transverse-field Ising model.

(iii) A further duality between a particular Majorana fermion architecture and a nearest-neighbor quantum spin $S = 1/2$ model which, in some sense, is intermediate between an Ising model on a honeycomb lattice and the Kitaev honeycomb model.[18] We term this system the "XXZ honeycomb compass model." This will allow us to illustrate that the classical version of this quantum XXZ honeycomb spin system is the classical three-dimensional (3D) Ising model in disguise. Similar results hold for a model of $(p + ip)$ superconducting grains on the checkerboard lattice.

Among the potential applications of the bond-algebraic formalism, we mention the following:

(i) The prospect of engineering topological quantum matter out of properly assembled Majorana networks. This is relevant for the potential realization of a topological quantum computer. We will outline a general procedure for the design of various architectures of nanowires on superconducting grains that support *topological quantum order* (TQO).[33] Our considerations will not be limited to the use of perturbation theory, e.g.,[20] but will rather rely on the use of symmetries and exact generalized dualities associated with these *granular* and other systems defined on general networks.

(ii) Viable assembly of quantum simulators out of Majorana networks to study, for instance, dynamics of quantum phase transitions. We show how to simulate the transverse-field Ising model chain and Hubbard-type models on the square lattice (which are shown to belong to the 3D Ising universality class).

As one of the key issues that we wish to address concerns viable TQO, boundary conditions may be of paramount importance. Boundary conditions are inherently related to the character (and, on highly connected systems, to the number) of independent d-dimensional gaugelike symmetries. Imposing periodic or other boundary conditions on a system can lead to vexing problems in traditional approaches to dualities and fermionization. By using bond algebras, we can circumvent these obstacles and construct exact dualities for both infinite systems and for finite systems endowed with arbitrary boundary conditions. Other formidable barricades, such as the use of nonlocal string transformations, can be overcome as well within the bond-algebraic approach to dualities.[31] The validity of any duality mapping can, of course, be checked numerically by establishing that the spectra of the two purported dual finite systems indeed coincide. The matching of the spectra serves as a definitive test since dualities are (up to global redundancies) unitary transformations[31] that preserve the spectrum of the system.

B. Outline

The remainder of this paper is organized as follows. In Sec. II, we briefly review recent work concerning Majorana nanowires on the square lattice. This discussion affords an introduction and motivation for the general architectures that we will discuss in this work. All sections that follow report on our original results. In Sec. III, we introduce a generalization of the square lattice architecture and consider an arbitrary network of superconducting grains and Majorana nanowires. This will lead us to consider a general high-dimensional interacting Majorana theory. In Sec. IV, we analyze the symmetries of our theory and discuss their implications for general observables, TQO, and autocorrelation times. In the few sections that follow, we will focus on our dualities (or high-dimensional fermionization). In Sec. V, we discuss dualities on general networks. We illustrate how our general interacting Majorana theories are dual to both QIG theories (Sec. V A) and to annealed quantum random transverse-field Ising models (Sec. V B). We discuss general physical implications of these dualities (including a duality between Ising gauge and quantum random transverse-field Ising models as well as the phase diagrams of the interacting Majorana theories) in Sec. V C. In Sec. VI, we derive several dualities for square lattice Majorana systems. We show that these are related to spin models on the honeycomb (Sec. VI A) and checkerboard (Sec. VI B) lattices. These dualities (especially perhaps our duality and consequent analysis for the honeycomb lattice quantum spin model) are somewhat unexpected and afford a counterpart to systems such as Kitaev's honeycomb model,[18] which exhibits lattice-direction-dependent spin interactions. In Sec. VII, we illustrate that, on the square lattice, *the standard Hubbard interaction term* in electronic systems is identical to the Majorana interactions in the theory that we analyze. By use of our dualities, this will allow us to prove that Hubbard-type

theories on the square lattice exhibit 3D Ising behavior. We further discuss how it may be possible to simulate the standard Hubbard model on the square lattice by a Majorana nanowire array. In Sec. VIII, we summarize our novel results. Certain technical details have been relegated to the Appendixes.

II. A REVIEW OF THE SQUARE LATTICE MAJORANA WIRE SYSTEM

In this section, following Ref. 20 we review a square lattice array of Josephson-coupled nanowires on superconducting grains. All of the results that we will report in all later sections of this article which follow this brief review are novel. A schematic of the array studied in Ref. 20 is presented in Fig. 1. As we will elaborate on in Sec. III, our general-dimensional extension of this Hamiltonian is given by Eqs. (5), (6), and (8) with c_{li} ($i = 1,2$) denoting Majorana operators [satisfying the standard Majorana algebra of Eq. (4)] associated with nanowire endpoints. Within the generalized scheme, these nanowires are placed on superconducting islands that occupy the vertices r of a general (even-coordinated) network, with links l connecting the islands. The ends of the nanowires are placed so that each link l connects two Majorana fermions c_{l1}, c_{l2} from different wires. Each link carries an arbitrary but fixed orientation, just for the purpose of labeling the Majoranas on it: As one traverses a link in the specified direction, c_{l1} comes before c_{l2} (see Fig. 1).

For example, in Fig. 1, two parallel nanowires are placed on each superconducting grain. These grains are placed on the sites r of a square lattice matrix. The two nanowires on each grain yield four Majorana fermionic degrees of freedom, placed on the edges of the oriented links of the
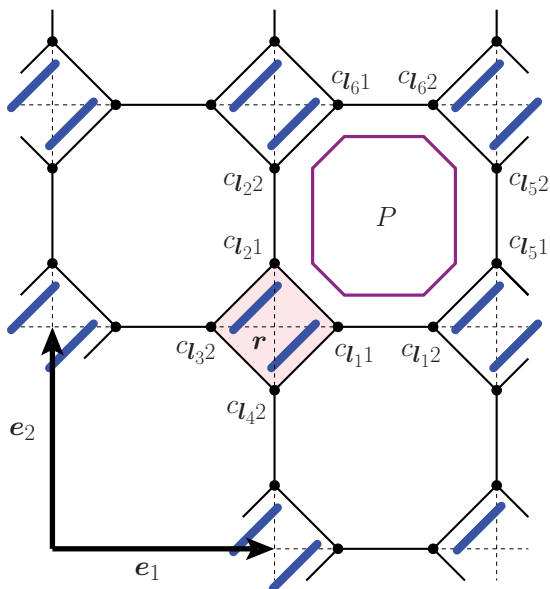

FIG. 1. (Color online) A decorated square lattice (with unit vectors e_1 and e_2) in which each site is replaced by a tilted square (representing a superconducting grain at site r). Two nanowires (solid blue diagonal lines) are placed on each grain. The grains are coupled to each other via Josephson couplings. A local (gauge) symmetry operator of the model is $G_P = (ic_{l_1 1} c_{l_1 2})(ic_{l_5 1} c_{l_5 2})(ic_{l_6 1} c_{l_6 2})(ic_{l_2 1} c_{l_2 2})$, where P defines the minimal closed loop. See text.

lattice. The Majorana fermions on different superconducting grains, sharing a link, are coupled to each other by Josephson junctions. Prior to introducing the Josephson couplings, each grain is shunted to maintain a fixed superconducting phase and is capacitively coupled to a ground plate. Consequently, there are large fluctuations in the electron-number operator. However, the electron-number parity is conserved. The sum of the two dominant effects is as follows: (i) intergrain Josephson couplings and (ii) intragrain constraints on the electron-number parity, complemented by exponentially small capacitive energies, leads to a simple effective Hamiltonian. The intragrain constraint on electron-number (even/odd) parity is more dominant than intergrain effects. The parity operator is $\mathcal{P}_r = (-1)^{n_r}$ with n_r the total number of electrons on grain r. This electron-number parity can be of paramount importance in interacting Majorana systems.[17,19] In grains having two nanowires each, the electronic parity operator is quartic in the Majorana fermions; it is just the ordered product of the four Majorana fermions at the endpoints of the nanowires on top of the grain at site r:

$$\mathcal{P}_r = c_{l_1 1} c_{l_2 1} c_{l_3 2} c_{l_4 2}, \quad r \in l_1, l_2, l_3, l_4 \qquad (1)$$

(we write $r \in l$ to indicate that r is one of the two endpoints of l). This gives rise to a term in the effective Hamiltonian of the form[20]

$$H_0 = -h \sum_r \mathcal{P}_r, \qquad (2)$$

with the sum taken over all grains, the total number of which is N_r. This term is augmented by Josephson couplings across intergrain links l, leading to a Majorana Fermi bilinear term involving the coupled pair of Majoranas $\{(c_{l1}, c_{l2})\}$,

$$H_1 = -J \sum_l ic_{l1} c_{l2}. \qquad (3)$$

Fermionic parity effects are more dominant than Josephson-coupling ($h \gg J$) effects. By invoking perturbation theory, for small (J/h), it was found[20] that, to lowest nontrivial order, the resultant effective Hamiltonian was identical to that of Kitaev's toric code model,[21] thus establishing that such a system may support TQO. Unfortunately, for (J/h) $\ll 1$, the spectral gap is small and the system is more susceptible to thermal fluctuations and noise. A Jordan-Wigner transformation was invoked[20] to illustrate that these results survive for finite (J/h).

III. GENERAL NETWORKS OF SUPERCONDUCTING GRAINS AND NANOWIRES

In Sec. II, we succinctly reviewed the effective Hamiltonian for the square lattice array,[20] depicted in Fig. 1, of Josephson-coupled granular superconductors carrying each two nanowires. This architecture serves as a useful case of study. *There is more to life, however, than square lattice arrays* (although we will return to these later on in this work). We consider next rather general architectures in which each node r (superconducting grain) has an even number of nearest neighbors to which it is linked by Josephson coupling (see Fig. 2). These general networks include, of course, any two-dimensional (2D) lattice of even coordination, e.g, those of Figs. 1 and 3, as special cases.
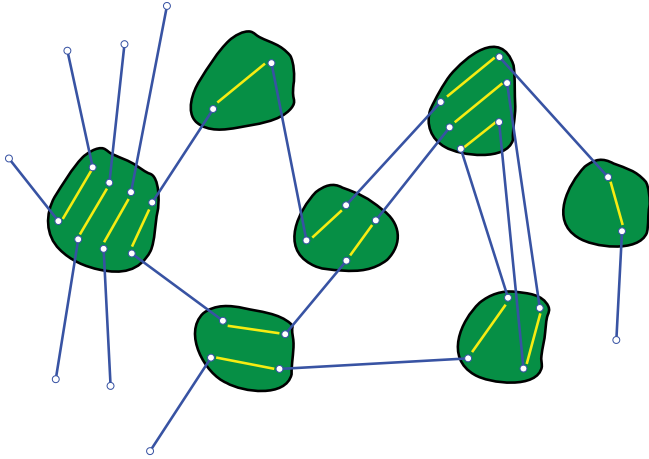
FIG. 2. (Color online) A general network of superconducting grains with an even coordination number of each vertex. The local coordination number q_r of any superconducting grain centered about site r is equal to the number of endpoints of all nanowires that are placed on that superconducting grain. The dominant Josephson tunneling paths between intergrain nanowire endpoints are highlighted by solid lines. Shown here is a two-dimensional projection of the network.

The architectures that we consider are realized by placing at each vertex r of a graph-theoretical network a finite-size superconducting grain. On each of these grains there are z_r nanowires. These nanowires provide $2z_r$ Majorana fermions, one for each wire's endpoint. Intergrain Josephson tunneling is represented by a link involving Majoranas coming from different wires on different islands. We place the nanowires on every grain in the network so that each endpoint of a nanowire is near the endpoint of another nanowire on a neighboring grain, to maximize Josephson tunneling. Thus, the coordination number q_r of grain r in these graphs is $q_r = 2z_r$.[34] The general situation is depicted in Fig. 2.

The basic inter-island and intra-island interactions have different origins. For ease of reference, we reiterate these below for arbitrary networks:

(i) there is a Josephson coupling J_l associated with each intergrain link l of the network connecting different superconducting grains, and
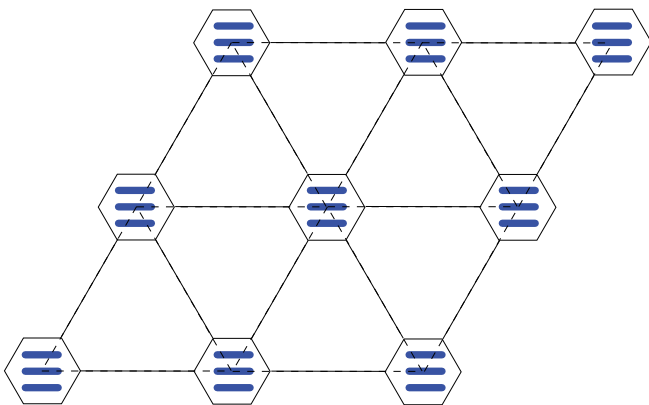

FIG. 3. (Color online) A triangular network of superconducting grains (hexagons) on each of which we place three nanowires.

(ii) an intragrain charging energy h_r associated to each island at site r.

In a general, spatially nonuniform, network the spatial distribution of couplings J_l and charging energies h_r need not be constant.

The algebra of Majorana fermions is defined by the following relations:

$$\{c_{li}, c_{l'i'}\} = 2\delta_{l,l'}\delta_{i,i'}, \quad c_{li}^\dagger = c_{li}. \tag{4}$$

With all of the above preliminaries in tow,[35] we are now ready to present the effective Hamiltonian for the systems under consideration,

$$H_{\rm M} = -i\sum_l J_l c_{l1} c_{l2} - \sum_r h_r \mathcal{P}_r, \tag{5}$$

where

$$\mathcal{P}_r \equiv i^{z_{r_2}} c_{l_1 i_1} c_{l_2 i_2} \ldots c_{l_{q_r} i_{q_r}}, \quad r \in l_1, \ldots, l_{q_r} \tag{6}$$

is the product of all Majorana fermion operators associated with the superconducting grain at site r, ordered in some definite but arbitrary fashion (differing orderings produce the same operator up to a sign).[36]

The index i_m can be either $i_m = 1$ or 2, depending on the particular orientation that has been assigned to the links in the network. More precisely, $i_m = 1$ if l_m points away from r, and $i_m = 2$ if l_m points into r. The factor $i^{z_{r_2}}$ is introduced to render $\mathcal{P}_r$ self-adjoint. Since

$$(c_{l_1 i_1} \ldots c_{l_{q_r} i_{q_r}})^\dagger = (-1)^{q_r(q_r-1)/2} c_{l_1 i_1} \ldots c_{l_{q_r} i_{q_r}} \tag{7}$$

and $q_r = 2z_r$, we set the integer z_{r_2} to be the number of nanowires counted modulo 2:

$$z_{r_2} = \begin{cases} 0 & \text{if} \quad z_r \text{ is even,} \\ 1 & \text{if} \quad z_r \text{ is odd.} \end{cases} \tag{8}$$

As we remarked earlier, the operators $\mathcal{P}_r$ are related to the operators n_r counting the total number of electrons on the grain r as

$$\mathcal{P}_r = (-1)^{n_r}, \tag{9}$$

thus measuring the *parity* of the number of electrons at site r. Hamiltonian (5) constitutes an arbitrary dimensional generalization of the sum of the two terms in Eqs. (2) and (3). In the following, we call the operators $\{ic_{l1}c_{l2}\}$ and $\{\mathcal{P}_r\}$ the *bonds* of the Hamiltonian $H_{\rm M}$.[30,31]

IV. TOPOLOGICAL QUANTUM ORDER IN MAJORANA NETWORKS

A notable question regarding systems of Majorana fermions is concerned with viable TQOs. We briefly summarize elements of TQO needed for this paper. Disparate (yet interrelated) definitions of TQO appear in the literature. One of the most striking (and experimentally important) aspects of TQO is its robustness against local perturbations or, equivalently, its inaccessibility to local probes at both zero and finite temperatures.[33] Some of the best-studied TQO systems are quantum Hall fluids.[22] Several lattice models are also well known to exhibit TQO, including the spin $S = 1/2$ models introduced by Kitaev.[18,21] As in our earlier works, we will use the

robustness or insensitivity to local probes[33] as our working definition of TQO. In the context of the Majorana lattice systems (and general networks) that we investigate here, one currently used approach for assessing the presence of TQO (Ref. 20) is observing whether a fortuitous match occurs, in perturbation theory, between (a) the studied nanowire systems with (b) Hamiltonians of lattice systems known to exhibit TQO. While such an analysis is highly insightful, it may be hampered by the limited number of lattice systems (and more general networks) that have already been established to exhibit TQO.

In this work, we suggest a different method for constructing Majorana system architectures displaying TQO. This approach does not require us to work towards an already examined lattice system that is known to exhibit TQO. Instead, our recipe invokes direct consequences of quantum invariances. Symmetries can mandate and protect the appearance of TQO (Ref. 33) via a generalization of Elitzur's theorem.[26,37] Specifically, whenever *d-dimensional gaugelike symmetries*[33] are present (most importantly, discrete $d = 1$ or continuous $d = 1, 2$ symmetries), finite-temperature TQO may be mandated. Zero-temperature TQO states protected by symmetry-based selection rules can be further constructed. A symmetry is termed a *d*-dimensional gaugelike symmetry if it involves operators/fields that reside in a *d*-dimensional volume.[26,33,37] The use of symmetries offers a direct route for establishing TQO that does not rely on particular known models as a crutch for establishing its presence.

For the particular case of the square lattice ($D = 2$), the interacting Majorana Hamiltonian H_M with periodic (toroidal) boundary conditions was found to exhibit 0-dimensional local, $d = 1$-dimensional gaugelike, and two-dimensional global symmetries.[20] These symmetries, inherently tied to TQO (Ref. 33) and dimensional reduction,[26,33,37] also appear in the more general network renditions of the granular system just described in the previous section. They are also manifest for the interacting Majorana systems embedded in any spatial dimension $D \geqslant 2$ when different boundary conditions are imposed.[38]

Global symmetry. The Hamiltonian H_M of Eq. (5) displays a global symmetry Q, given by the product of all the Majorana fermion operators in the system. We can write Q in terms of bonds as

$$Q = \prod_r \mathcal{P}_r, \tag{10}$$

since each Majorana is contributed by some island. The order of the bonds in Q is not an issue since

$$[\mathcal{P}_r, \mathcal{P}_{r'}] = 0 \tag{11}$$

for any pair of sites r, r'. The conserved charge Q represents a $\mathbb{Z}_2$ symmetry of the system,

$$Q^2 = \mathbb{1}. \tag{12}$$

Beyond this global symmetry, the system of Eq. (5) exhibits independent symmetries that operate on finer, lower-dimensional regions of the network. Of particular importance to TQO are $d = 1$- and $d = 0$-dimensional symmetries, and so we turn to these next.

$d = 1$ symmetries. The $d = 1$-dimensional symmetry operators of the Majorana system are given by

$$Q_\ell = \prod_{l \in \ell} (i c_{l1} c_{l2}), \quad (Q_\ell)^2 = \mathbb{1}, \tag{13}$$

where ℓ is a continuous contour, finite or infinite and open or closed depending on boundary conditions, entirely composed of links. That these nonlocal operators are symmetries is readily seen once it is noted that (a) each of the terms (or *bonds*) in the summand of Eq. (5) defining H_M involves products of an even number of Majorana fermions and (b) by the second of Eqs. (4), effecting an even number of permutations of Majorana fermion operators in a product incurs no sign change. For example, for a network of linear dimension L along a Cartesian axis, the contour ℓ spans $\mathcal{O}(L^1)$ sites and is thus a $d = 1$-dimensional object. This is the origin of the name $d = 1$ symmetries. Some of these $d = 1$ symmetries may be related to (appear as products of) the local symmetries discussed next, depending on the topology enforced by boundary conditions. Some others are fundamental and can not be expressed in terms of those local symmetries.

$d = 0$ symmetries. For the models under consideration, local, also called gauge, $d = 0$ symmetries are associated with the elementary loops (or plaquettes) P of the wires (see Fig. 1 for an example). That is, when considering the superconductors as point nodes, the links l form a network with minimal closed loops P. The associated local symmetries are given by

$$G_P = \prod_{l \in P} (i c_{l1} c_{l2}), \quad G_P^2 = \mathbb{1}. \tag{14}$$

Repeating the considerations of (a) and (b) above, we see that, for any elementary plaquette P, the product of Majorana fermion operators in Eq. (14) commutes with H_M since it shares an even number (possibly zero) of Majorana fermions with any bond in the Hamiltonian. By multiplying operators G_P for a collection of plaquettes P that, together, tile a region bounded by the loop Γ, it is readily seen that this product is also a symmetry, as in standard theories with gauge symmetries.

The symmetries above lead to nontrivial physical consequences: (a) By virtue of Elitzur's theorem[39] and its $d > 0$ generalizations,[26,33,37] all nonvanishing correlators $\langle \prod_{\alpha \in S} c_\alpha \rangle$ with S a set of indices α must be invariant under all of the symmetries of Eqs. (13) and (14). That is, $d = 0, 1$ gaugelike symmetries can not be spontaneously broken. As we alluded to earlier, one consequence of the nonlocal symmetries such as the $d = 1$ symmetries of Eq. (13) is the existence of TQO.[33,38] (b) Bounds on autocorrelation times. As a consequence of the $d = 1$ symmetries of Eq. (13), and the aforementioned generalization of Elitzur's theorem as it pertains to temporal correlators,[26] the Majorana fermion system will exhibit finite autocorrelation times regardless of the system size. Of course, for various realizations of dynamics and geometry of the disorder, different explicit forms of the autocorrelation times τ can be found. For instance, by use of bond algebras, Kitaev's toric code model is identical to that of a classical square plaquette model as in Ref. 40. Similarly, Kitaev's toric code model[21] can be mapped onto two uncoupled one-dimensional Ising chains.[27,28,33] Different realizations of the dynamics can lead to different explicit forms of τ in both cases, however,

finite autocorrelation times are found in all cases (as they must be). Similarly, more general than the exact bond-algebraic mapping and dimensional reductions that we find here, by virtue of $d = 1$ symmetries of Eq. (13), autocorrelation functions involving Majorana fermions on a line ℓ must be bounded by corresponding ones in a $d = 1$-dimensional system.[26]

V. ARBITRARY-DIMENSIONAL MAJORANA ARCHITECTURES

In this section, we provide two spin duals to the interacting Majorana system described by the effective Hamiltonian H_M of Eq. (5) on arbitrary lattices/networks. This applies to finite or infinite systems and for arbitrary boundary conditions. These two dual systems are (1) QIG theories for $D = 2$ systems, and more general spin gauge theories in higher dimensions, and (2) a family of transverse-field Ising models with annealed disorder in the exchange couplings (each model representing a single gauge sector of H_M). The dualities will be established in the framework of the theory of bond algebras of interactions,[30,31] as it applies to the study of general dualities between many-body Hamiltonians. The general bond-algebraic method relies on a comparison of the algebras, in the respective two dual model, that are generated by the corresponding local interaction terms (or *bonds*) in these theories.[26–32] For the problem at hand, the Hamiltonian H_M is built as the sum of two sets of Hermitian bonds

$$ic_{l1}c_{l2}, \quad \mathcal{P}_r, \tag{15}$$

where l and r are links and sites of the network supporting H_M [$\mathcal{P}_r$ was defined in Eq. (6)]. In this paper, we will only consider the bond algebra $\mathcal{A}_M$ generated by these bonds. We can then obtain dual representations of H_M by looking for alternative local representations of $\mathcal{A}_M$. But, first we have to characterize $\mathcal{A}_M$ in terms of relations.

The problem of characterizing a bond algebra of interactions is simplified by several features brought about by physical considerations of locality. The first consequence of locality is that interactions are *sparse*, meaning that each bond in any local Hamiltonian commutes with most other bonds and is involved in only a small number of relations (or constraints) that link individual bonds to one another. Hence, the number of nontrivial relations per bond is small. The second consequence is that relations in a bond algebra can be classified into intensive and extensive, and most relations are intensive. We call a relation *intensive* if the number of bonds it involves is *independent of the size of the system*, and extensive if the numbers of bonds it involves scales with the size of the system. Since extensive relations could potentially lead to unphysical nonlocal behavior, they are typically few in number and may reflect the topology of the system regulated by the boundary conditions, as we will illustrate repeatedly in this paper. As there are ($2z_r$) Majorana modes (or, equivalently, z_r fermionic modes) per grain, the Majorana theory of Eq. (5) and the algebraic relations listed above are defined on a Hilbert space of dimension $\dim \mathcal{H}_M = 2^{z_r N_r}$

Next, we characterize the bond algebra $\mathcal{A}_M$ as the first step toward the construction of its spin duals. The intensive

relations are as follows:

(1) for any r and l

$$(ic_{l1}c_{l2})^2 = \mathbb{1} = (\mathcal{P}_r)^2, \tag{16}$$

(2) for $r, r' \in l$,

$$\{\mathcal{P}_r, ic_{l1}c_{l2}\} = 0 = \{\mathcal{P}_{r'}, ic_{l1}c_{l2}\}, \tag{17}$$

(3) for $r \in l_i$, $i = 1, 2, \ldots, q_r$,

$$\{\mathcal{P}_r, ic_{l_i1}c_{l_i2}\} = 0. \tag{18}$$

Thus, in the bulk, or everywhere for periodic boundary conditions, each island anticommutes with q_r (the coordination of r) links, and each link anticommutes with two islands. The presence or absence of extensive relations depends on the boundary conditions. For periodic (toroidal) or other closed boundary conditions (e.g., spherical), we have one extensive relation

$$\prod_r \mathcal{P}_r = \alpha \prod_l (ic_{l1}c_{l2}), \quad \alpha = \pm 1 \tag{19}$$

since each Majorana fermion operator appears exactly once both on the left- and right-hand sides of this equation, but not necessarily in the same order. The constant α adjusts for the potentially different orderings, and the overall powers of i on each side of the equation. Notice that $\prod_r \mathcal{P}_r = Q$ is the global $\mathbb{Z}_2$ symmetry operator. In contrast, for open or semiopen (e.g., cylindrical) boundary conditions, the islands on the free boundary have Majorana fermions that are not matched by links (that is, that do not interact with Majoranas on other islands). Hence, the product

$$\left(\prod_r \mathcal{P}_r\right)\left(\prod_l (ic_{l1}c_{l2})\right) = B \tag{20}$$

reduces to the product B of these Majoranas on the free boundary. The operator B may or may not commute with the Hamiltonian, depending on the details of the architecture at the boundary (see Fig. 4), but either way Eq. (20) does not represent an extensive relation in the bond algebra (rather it
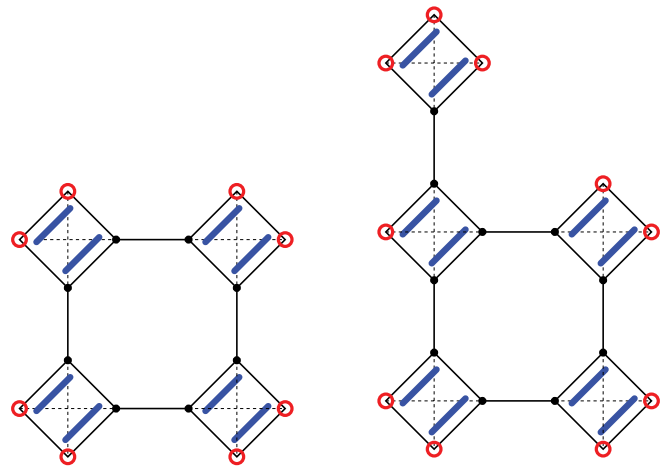

FIG. 4. (Color online) Two architectures with open boundary conditions. In either case, the operator B of Eq. (20) is the product of all the uncoupled Majoranas on the boundary indicated by open circles, but $[H_M, B] = 0$ only for the system shown in the panel on the left.

just states how to write a particular operator as a product of bonds). If $[H_M, B] = 0$, B represents a $\mathbb{Z}_2$ boundary symmetry independent of the local symmetries.

A. Duality to quantum Ising gauge theories

In this section, we describe a duality relating the Hamiltonian H_M to a system of $S = 1/2$ spins. The spin degrees of freedom are placed on the (center of the) *links* of a network identical to the one associated to H_M, and are described by Pauli matrices $\sigma_l^x, \sigma_l^y, \sigma_l^z$. The goal is to introduce interactions among these spins that satisfy the same algebraic relations as the bonds of H_M. Let us introduce the Hermitian spin bond (a plaquette operator)

$$\widetilde{\mathcal{P}}_r = \prod_{\{l|r \in l\}} \sigma_l^z. \tag{21}$$

For example, for the special case of the square lattice discussed in the Introduction,

$$\widetilde{\mathcal{P}}_r = \sigma_{l_1}^z \sigma_{l_2}^z \sigma_{l_3}^z \sigma_{l_4}^z, \quad r \in l_1, l_2, l_3, l_4. \tag{22}$$

On general planar graphs, the set of spin bonds

$$\sigma_l^x, \quad \widetilde{\mathcal{P}}_r, \tag{23}$$

satisfy the following intensive relations:

(1) for any r and l,

$$\left(\sigma_l^x\right)^2 = \mathbb{1} = (\widetilde{\mathcal{P}}_r)^2, \tag{24}$$

(2) for $r, r' \in l$,

$$\{\widetilde{\mathcal{P}}_r, \sigma_l^x\} = 0 = \{\widetilde{\mathcal{P}}_{r'}, \sigma_l^x\}, \tag{25}$$

(3) for $r \in l_i$, $i = 1, 2, \ldots, q_r$,

$$\{\widetilde{\mathcal{P}}_r, \sigma_{l_i}^x\} = 0, \tag{26}$$

everywhere for closed boundary conditions, and everywhere in the bulk for open or semiopen boundary conditions. These relations are identical to the intensive relations for the bonds of H_M.[41] In the Ising gauge theory, the bond-algebraic relations listed above are defined on a space of size $2^{z_r N_r}$. (That this is so can be easily seen by noting that there are $N_l = z_r N_r$ links each endowed with a spin $S = 1/2$ degree of freedom σ_l^z.) As it so happens, this Hilbert space dimension is identical to that of the Majorana system of H_M. Putting all of the pieces together, we see that the spin Hamiltonian

$$H_{QIG} = -\sum_l J_l \sigma_l^x - \sum_r h_r \widetilde{\mathcal{P}}_r \tag{27}$$

is *unitarily equivalent* to H_M, provided the extensive relations are matched as well. For open or semiopen boundary conditions, the same follows provided that the intensive relations on the boundary also properly match. In the following, we focus on periodic boundary conditions (of theoretical interest in connection to TQO), and leave the discussion of open boundary conditions (of interest for potential experimental realizations of these systems) to Appendix A. We remark that more standard Majorana fermion representations of spins, similar to those discussed in Appendix B, do not lead to the simple dualities that we now derive.

As just explained, the mapping of bonds

$$ic_{l1}c_{l2} \mapsto \sigma_l^x, \quad \mathcal{P}_r \mapsto \widetilde{\mathcal{P}}_r \tag{28}$$

preserves the intensive algebraic relations. In particular, it maps the local symmetries of Eq. (14) to local symmetries of H_{QIG},

$$G_P \equiv \prod_{l \in P} (ic_{l1}c_{l2}) \mapsto \prod_{l \in P} \sigma_l^x \equiv G_{S,P}. \tag{29}$$

To assess the effect it has on the extensive relation of Eq. (19) (and the global symmetry), notice that (for periodic boundary conditions)

$$\prod_l (ic_{l1}c_{l2}) \mapsto \prod_l \sigma_l^x \equiv Q_S \tag{30}$$

with $[Q_S, H_{QIG}]$ a global symmetry of H_{QIG}, and

$$\prod_r \mathcal{P}_r \mapsto \prod_r \widetilde{\mathcal{P}}_r = \mathbb{1}. \tag{31}$$

It follows that, as it stands, the mapping of bonds of Eq. (28) is a correspondence, but not an *isomorphism* of bond algebras. The simplest way to convert it into an isomorphism is to modify one and only one of the bonds $\widetilde{\mathcal{P}}_r$ of the spin model at some arbitrary site r_0, so that

$$\widetilde{\mathcal{P}}_{r_0} \equiv \alpha Q_S \prod_{\{l|r_0 \in l\}} \sigma_l^z \tag{32}$$

[α was defined in Eq. (19)], while for any other site $r \neq r_0$, $\widetilde{\mathcal{P}}_r$ remains unchanged. The introduction of this modified bond does not change the intensive relations since Q_S commutes with every bond (original or modified). Moreover,

$$\prod_r \mathcal{P}_r \mapsto \widetilde{\mathcal{P}}_{r_0} \prod_{r \neq r_0} \widetilde{\mathcal{P}}_r = \alpha Q_S \tag{33}$$

and the extensive relation of Eq. (19) is now, with the modified definition of $\widetilde{\mathcal{P}}_{r_0}$, preserved since ($\alpha^2 = 1$)

$$\prod_l \sigma_l^x = \alpha \widetilde{\mathcal{P}}_{r_0} \prod_{r \neq r_0} \widetilde{\mathcal{P}}_r. \tag{34}$$

Hence, there is a unitary transformation $\mathcal{U}_d$ such that

$$\mathcal{U}_d H_M \mathcal{U}_d^\dagger = H_{QIG}, \tag{35}$$

with H_{QIG} containing the single modified bond $\widetilde{\mathcal{P}}_{r_0}$.

In the duality between the systems of Eqs. (5) and (27), the dimensions of the their Hilbert spaces are identical. Since we count two Majorana modes (or, equivalently, one fermionic mode) per link, the Hamiltonian H_M is defined on a Hilbert space of dimension $\dim \mathcal{H}_M = 2^{N_l}$, with N_l denoting the total number of links in the network. On the other hand, the spin system has one spin $S = 1/2$ degree of freedom per link, hence the dimension of the Hilbert space on which H_{QIG} is defined is also 2^{N_l}. Notice that the need to introduce the modified bond $\widetilde{\mathcal{P}}_{r_0}$ in the dual-spin theory is irrelevant from the point of exploiting the duality to study the ground-state properties of H_M (or *vice versa*, to study the ground-state properties of H_{QIG}) since for finite systems the ground state $|\Omega\rangle$ must satisfy $Q_S|\Omega\rangle = |\Omega\rangle$. The ease with which we established the duality between Majorana systems and QIG systems for general lattices and networks illustrates how efficient the bond-algebraic construct is.

The duality just described is extremely general, valid in particular for any number of space dimensions D. In the following, we describe explicitly one particularly important special instance, that of $D = 2$. On a square lattice, the
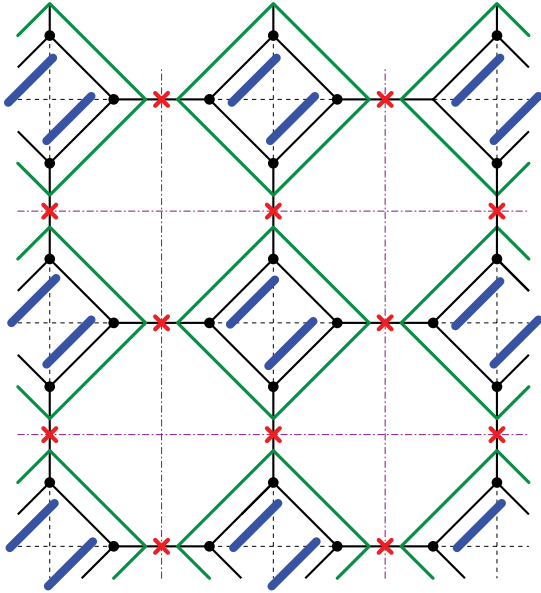
FIG. 5. (Color online) Duality to a $D = 2$ $\mathbb{Z}_2$ QIG theory, where spins are represented as crosses. Hamiltonian H_M of Eq. (36) represents a particular fermionization of H_{QIG}.

Hamiltonian H_M simplifies to

$$H_M = -\sum_l J_l(ic_{l1}c_{l2}) - \sum_r h_r c_{l_{11}}c_{l_{21}}c_{l_{32}}c_{l_{42}}, \quad (36)$$

where l_1, l_2, l_3, l_4 are shown in Fig. 1. This generalizes the Hamiltonian considered in Ref. 20 only in that inhomogeneous couplings are allowed. The dual-spin (finite-size) system is ($r_0 \in l_{0,1}, l_{0,2} l_{0,3} l_{0,4}$)

$$H_{QIG} = -h_{r_0}\alpha Q_S \sigma^z_{l_{0,1}}\sigma^z_{l_{0,2}}\sigma^z_{l_{0,3}}\sigma^z_{l_{0,4}} - \sum_{r \neq r_0} h_r \sigma^z_{l_1}\sigma^z_{l_2}\sigma^z_{l_3}\sigma^z_{l_4}$$
$$- \sum_l J_l \sigma^x_l \quad (37)$$

that we recognize as the standard, $D = 2$, $\mathbb{Z}_2$ QIG theory,[42] up to the modified bond at r_0 [$Q_S = \prod_l \sigma^x_l$ and α is determined according to Eq. (19)] (see Fig. 5).

Hence, we may regard the Hamiltonian of Eq. (36) as an exact fermionization of the $\mathbb{Z}_2$ QIG theory with periodic boundary conditions (and one modified bond). It is interesting to compare this fermionization with a slightly different one[25] that exploits the Jordan-Wigner transformation in the limit of infinite size. This approach yields the Majorana Hamiltonian[25] (in our notation)

$$H_{FSS} = -\sum_l J_l(ic_{l1}c_{l2}) - \sum_r h_r c_{l_{12}}c_{l_{51}}c_{l_{62}}c_{l_{21}}, \quad (38)$$

where l_1, l_2, l_5, l_6 are shown in Fig. 1. *The two-body interaction $c_{l_{12}}c_{l_{51}}c_{l_{62}}c_{l_{21}}$ is different than the two-body interaction in H_M since it involves three different islands* (see Fig. 6). Hence, disregarding boundary conditions, we see that the $\mathbb{Z}_2$ QIG theory admits rather different but equivalent fermionizations. As expected, the bonds in H_{FSS} satisfy intensive relations identical to those already discussed for H_M and H_{QIG}. However, contrary to what is claimed in Ref. [20] Hamiltonian H_{FSS} is not the same as the Hamiltonian of Eq. (5) which is the one relevant for Majorana architectures.[43]
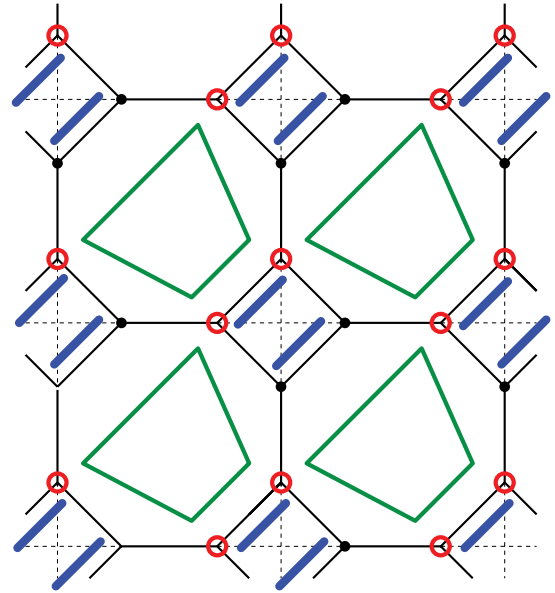

FIG. 6. (Color online) Jordan-Wigner fermionization of the $\mathbb{Z}_2$ QIG theory realizes a theory of Majorana fermions H_{FSS}, with two-body interactions between Majoranas (shown as trapezoids) on three different islands. Notice that, unlike the intra-island two-body interactions of H_M, two neighboring two-body interactions H_{FSS} share a Majorana operator.

Thus far, we focused on periodic boundary conditions. We now remark on other boundary conditions. When antiperiodic boundary conditions are imposed in a network with an an outer perimeter that includes twice an odd number of links, the right-hand side of Eq. (31) is replaced by $-\mathbb{1}$. The union of both cases (periodic and antiperiodic) for a system having a twice-odd perimeter spans all possible values of the product $\prod_r \widetilde{\mathcal{P}}_r$. Thus, for these systems in the case of periodic boundary conditions, the spectrum of the Majorana system can be mapped to the union of levels found for the QIG systems for both periodic or antiperiodic boundary conditions. In terms of the corresponding partition functions, we have that

$$\mathcal{Z}_{M, \text{periodic}} = \mathcal{Z}_{QIG, \text{periodic}} + \mathcal{Z}_{QIG, \text{antiperiodic}}. \quad (39)$$

B. Duality to annealed transverse-field Ising models

We next derive, in a similar spirit, a duality between the general architecture Majorana system H_M and annealed transverse-field Ising models. The number of annealed disorder variables in these systems (along with the number of sites N_r) determines the size of the Hilbert space on which the Ising models are defined. With an eye towards things to come, we note (as we will reiterate later on) that the duality that we will derive in this section will furnish an example in which the Hilbert space dimensions of two dual systems need not be identical to one another. Generally, dualities are unitary transformations between two theories up to trivial gauge redundancies that do not preserve the Hilbert space dimension.[31] That is, dualities are isometries.

To define the annealed transverse-field Ising systems, we place an $S = 1/2$ spin on each site r, $\sigma^x_r, \sigma^y_r, \sigma^z_r$ of the network associated to H_M, and a *classical* annealed disorder variable

$\eta_l = \pm 1$ on each link l. Then, we can introduce the set of Hermitian spin bonds

$$\sigma_{\boldsymbol{r}}^x, \quad \eta_l \sigma_{\boldsymbol{r}}^z \sigma_{\boldsymbol{r}'}^z, \quad \boldsymbol{r}, \boldsymbol{r}' \in l. \tag{40}$$

If we specialize to periodic boundary conditions, these bonds satisfy a set of intensive relations identical to those discussed in the two previous sections, together with *one* relation absent before and listed last below:

(1) for any $\boldsymbol{r}$ and l

$$\left(\sigma_{\boldsymbol{r}}^x\right)^2 = \mathbb{1} = \left(\eta_l \sigma_{\boldsymbol{r}}^z \sigma_{\boldsymbol{r}'}^z\right)^2, \tag{41}$$

(2) for $\boldsymbol{r}, \boldsymbol{r}' \in l$

$$\left\{\sigma_{\boldsymbol{r}}^x, \eta_l \sigma_{\boldsymbol{r}}^z \sigma_{\boldsymbol{r}'}^z\right\} = 0 = \left\{\sigma_{\boldsymbol{r}'}^x, \eta_l \sigma_{\boldsymbol{r}}^z \sigma_{\boldsymbol{r}'}^z\right\}, \tag{42}$$

(3) for $\boldsymbol{r} \in l_i$, $i = 1, 2, \dots, q_{\boldsymbol{r}}$,

$$\left\{\sigma_{\boldsymbol{r}}^x, \eta_{l_i} \sigma_{\boldsymbol{r}}^z \sigma_{\boldsymbol{r}'_i}^z\right\} = 0, \quad \boldsymbol{r} \neq \boldsymbol{r}'_i \in l_i, \tag{43}$$

(4) for any elementary loop P in the network,

$$\prod_{l \in P} \left(\eta_l \sigma_{\boldsymbol{r}}^z \sigma_{\boldsymbol{r}'}^z\right) = \mathbb{1} \prod_{l \in P} \eta_l. \tag{44}$$

The constraint of Eq. (44) holds true for any closed loop. For this reason, and others related to TQO, it is important to clarify the meaning of *elementary loop*.

Loops in the network that share some links can be joined along those links to obtain another loop or sum of disjoint loops. This means that the set of all loops has a minimal set of generators from which we can obtain any loop or systems of loops by the joining operation just described. We call the loops in an arbitrary but fixed minimal generating set *elementary loops*. In this way, we obtain a minimal description of the constraints embodied in Eq. (44). It is not obvious *a priori* whether one should classify these constraints (that is, relations) as intensive or extensive. This depends on the topology of the system. If the system is simply connected, every loop is contractible to some trivial minimal (that is, of minimal length) loop, and hence we can choose minimal loops as elementary loops. These loops afford an intensive characterization of the constraints embodied in Eq. (44). If, on the other hand, the system is not simply connected, as for periodic boundary conditions, the generating set of elementary loops will include noncontractible loops, and the length of some of these noncontractible loops may scale with the size of the system. Consider, for example, the spin bonds of Eq. (40) on a planar network on the torus and on a punctured infinite plane. Both networks fail to be simply connected, but only the torus forces some of the constraint of Eq. (44) to be extensive because its two noncontractible loops must scale with the size of the system.

For periodic boundary conditions, there is one extensive relation satisfied by the bonds of Eq. (40):

$$\prod_l \left(\eta_l \sigma_{\boldsymbol{r}}^z \sigma_{\boldsymbol{r}'}^z\right) = \eta \mathbb{1}, \tag{45}$$

with

$$\eta \equiv \prod_l \eta_l, \quad \eta = \pm 1, \tag{46}$$

which may or may not be independent of the relations of Eq. (44), depending on the details of the network. In the
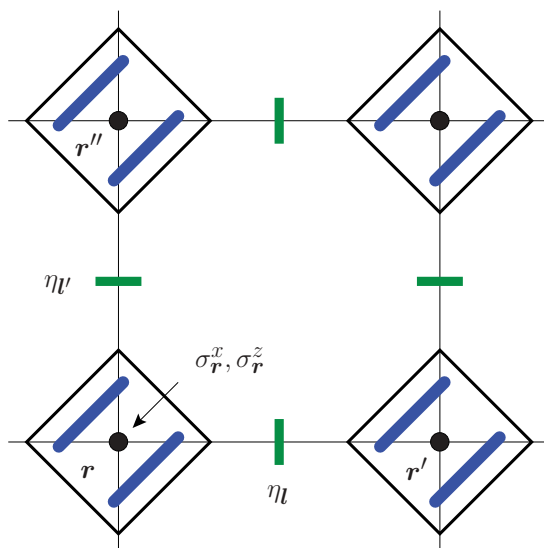

FIG. 7. (Color online) Duality to an annealed transverse-field Ising model, in the particular $D = 2$ case. Spins $S = 1/2$ are located at the vertices $\boldsymbol{r}$ of the square lattice and classical $\mathbb{Z}_2$ fields η_l at the links l (indicated by a dash).

following, we will treat it as an independent relation since it does not affect our results if it turns out to be dependent.

It follows that the mapping of bond algebras

$$ic_{l1}c_{l2} \mapsto \eta_l \sigma_{\boldsymbol{r}}^z \sigma_{\boldsymbol{r}'}^z, \quad \mathcal{P}_{\boldsymbol{r}} \mapsto \sigma_{\boldsymbol{r}}^x \tag{47}$$

preserves every local anticommutation relation. Hence, the Hamiltonian theory

$$H_{\mathrm{AI}}\{\eta_l\} = -\sum_l J_l \left(\eta_l \sigma_{\boldsymbol{r}}^z \sigma_{\boldsymbol{r}'}^z\right) - \sum_{\boldsymbol{r}} h_{\boldsymbol{r}} \sigma_{\boldsymbol{r}}^x, \tag{48}$$

obtained from applying this mapping to H_{M}, will be shown to be dual to H_{M} (see Fig. 7). The Hilbert space on which the theory of Eq. (48) is defined is of size $\dim \mathcal{H}_{\mathrm{AI}} = 2^{N_{\boldsymbol{r}} + N_\eta}$ where $N_{\boldsymbol{r}}$ is the number of superconducting grains and N_η the total number of η_l fields.

The proposed duality raises an immediate question: What are the features of H_{M} that determine or at least constrain the classical fields η_l? As we will see, the answer lies in the local and gaugelike symmetries that H_{M} possesses and H_{AI} lacks. To understand this better, we need to study the effect this mapping has on relations beyond local anticommutation. Let us consider first its effect on the extensive relation of Eq. (19). We have that

$$Q = \prod_{\boldsymbol{r}} \mathcal{P}_{\boldsymbol{r}} \mapsto \prod_{\boldsymbol{r}} \sigma_{\boldsymbol{r}}^x = Q_S, \tag{49}$$

$$\alpha \prod_l (ic_{l1}c_{l2}) \mapsto \alpha \prod_l \left(\eta_l \sigma_{\boldsymbol{r}}^z \sigma_{\boldsymbol{r}'}^z\right) = \alpha \eta \mathbb{1}. \tag{50}$$

As for periodic boundary conditions, the left-hand sides of Eqs. (49) and (50) represent the same operator, but the right-hand sides are different operators, and the mapping as it stands does not preserve the relation of Eq. (19). We know of a solution to this shortcoming from the previous section. If we modify one and only one bond placed on some fixed but arbitrary link l_0 to read as

$$\alpha \eta \eta_{l_0} \sigma_{\boldsymbol{r}}^z \sigma_{\boldsymbol{r}'}^z Q_S, \tag{51}$$

then

$$\alpha \prod_l (ic_{l1}c_{l2}) \mapsto \alpha^2 \left(\eta \eta_{l_0} \sigma_{\boldsymbol{r}_0}^z \sigma_{\boldsymbol{r}_{0'}}^z\right) Q_S \prod_{l \neq l_0} \left(\eta_l \sigma_{\boldsymbol{r}}^z \sigma_{\boldsymbol{r}'}^z\right) = Q_S, \tag{52}$$

as required by Eq. (19).

The presence of the modified bond at $\boldsymbol{l}_0$ introduces a new feature into the discussion leading to Eq. (44). Now we have that, for any elementary loop P,

$$\prod_{l \in P} \left(\eta_l \sigma_{\boldsymbol{r}}^z \sigma_{\boldsymbol{r}'}^z\right) = \begin{cases} \mathbb{1} \prod_{l \in P} \eta_l & \text{if } \boldsymbol{l}_0 \notin P, \\ \alpha \eta Q_S \prod_{l \in P} \eta_l & \text{if } \boldsymbol{l}_0 \in P. \end{cases} \tag{53}$$

If we consider the role of the elementary loops P in the Majorana system H_{M}, and consider the mapping of Eq. (40), we see that the local symmetries (see Sec. IV)

$$G_P \equiv \prod_{l \in P} (ic_{l1}c_{l2}) \tag{54}$$

of H_{M} are mapped to one of the two possibilities listed in Eq. (53), showing that, as it stands, the mapping of Eq. (40) is still not an isomorphism of bond algebras. The problem is that a large number of distinct symmetries are being mapped either to a trivial symmetry (a multiple of the identity operator), or a multiple of the global $\mathbb{Z}_2$ symmetry Q_S of the annealed Ising model. We can fix this problem by decomposing the Hamiltonians H_{M} and H_{AI} into their symmetry sectors, where the obstruction to the duality mapping disappears. Thus, we are able to establish *emergent dualities*,[30,31] that is, dualities that emerge between *sectors* of the two theories.

The sector decomposition is simple for H_{AI}, which has only one symmetry Q_S, with eigenvalues $q_S = \pm 1$. Then, we can decompose the Hilbert space $\mathcal{H}_{\mathrm{AI}}$ as

$$\mathcal{H}_{\mathrm{AI}} = \bigoplus_{q_S = \pm 1} \mathcal{H}_{q_S}, \tag{55}$$

so that if Λ_{q_S} is the orthogonal projector onto $\mathcal{H}_{q_S}$, then

$$Q_S \Lambda_{q_S} = \pm \Lambda_{q_S}. \tag{56}$$

For H_{M}, since its symmetries form a commuting set, one can simultaneously diagonalize them and break the Hilbert space $\mathcal{H}_{\mathrm{M}}$ into sectors labeled by the symmetries' simultaneous eigenvalues, $q = \pm 1$ for the global symmetry and $\Gamma_P = \pm 1$ for the loop symmetries:

$$\mathcal{H}_{\mathrm{M}} = \bigoplus_{q, \{\Gamma_P\}} \mathcal{H}_{q, \{\Gamma_P\}}. \tag{57}$$

The Hamiltonian H_{M} is block diagonal relative to this decomposition, and, if $\Lambda_{q, \{\Gamma_P\}}$ is the orthogonal projector onto the subspace $\mathcal{H}_{q, \{\Gamma_P\}}$, we have that

$$Q \Lambda_{q, \{\Gamma_P\}} = q \Lambda_{q, \{\Gamma_P\}}, \tag{58}$$

$$G_P \Lambda_{q, \{\Gamma_P\}} = \Gamma_P \Lambda_{q, \{\Gamma_P\}} \tag{59}$$

for any elementary loop P.

The problem now is to decide which choice of sectors will make the projected Hamiltonians $H_{\mathrm{M}} \Lambda_{q, \{\Gamma_P\}}$ and $H_{\mathrm{AI}} \Lambda_{q_S}$ dual to each other. From Eqs. (49) and (53), we obtain the

relations

$$q = q_S, \tag{60}$$

$$\Gamma_P = \begin{cases} \prod_{l \in P} \eta_l & \text{if } \boldsymbol{l}_0 \notin P, \\ \alpha \eta q_s \prod_{l \in P} \eta_l & \text{if } \boldsymbol{l}_0 \in P, \end{cases} \tag{61}$$

which allow us to connect the two theories

$$U_{\mathrm{d}} H_{\mathrm{M}} \Lambda_{q, \{\Gamma_P\}} U_{\mathrm{d}}^\dagger = H_{\mathrm{AI}} \{\eta_l\} \Lambda_{q_s}, \tag{62}$$

where the unitary transformation U_{d} implements an *emergent duality* that holds only on the indicated sectors of the two theories.

The dual-spin representation of H_{M} projected onto the gauge-invariant sector $q = 1, \{\Gamma_P = 1\}$ is given by the inhomogeneous Ising model ($\eta_l = 1$ on every link)

$$H_{\mathrm{AI}} \{1\} = -\sum_l J_l \sigma_{\boldsymbol{r}}^z \sigma_{\boldsymbol{r}'}^z - \sum_{\boldsymbol{r}} h_{\boldsymbol{r}} \sigma_{\boldsymbol{r}}^x, \tag{63}$$

and is known as a *gauge-reducing duality*.[31] For the special case of the square lattice and homogeneous couplings, one would expect that this sector contains the ground state of H_{M}.

C. Physical consequences

We have by now seen, on general networks in an arbitrary number of dimensions, that ordinary QIG theories (and their generalizations) and annealed transverse-field Ising models arise from the very same Majorana system when it is dualized in different ways. Therefore, by transitivity,

$$H_{\mathrm{QIG}} \overset{\text{dual}}{\longleftrightarrow} H_{\mathrm{AI}}. \tag{64}$$

This correspondence leads to several consequences. In its simplest incarnation, that for $D = 2$ Majorana networks, this duality connects, via an imaginary-time transfer matrix (or τ-continuum limit) approach,[31,44] disordered $D = 3$ classical Ising models to $D = 3$ classical Ising gauge theories. In its truly most elementary rendition among these planar networks, that of the square lattice, the duality of Eq. (64) implies that the effect of the bimodal annealed disordering fields $\eta_l = \pm 1$ is immaterial in determining the universality class of the system. This is so as the standard random transverse-field Ising model on the square lattice

$$H_{\mathrm{RTFIM}} = -\sum_l J_l \sigma_{\boldsymbol{r}}^z \sigma_{\boldsymbol{r}'}^z - \sum_{\boldsymbol{r}} h_{\boldsymbol{r}} \sigma_{\boldsymbol{r}}^x \tag{65}$$

[i.e., Eq. (48) in the absence of annealed bimodal disorder] similarly maps, via a transfer-matrix approach, onto a corresponding classical Ising model on a cubic lattice. The uniform transverse-field Ising model (that with uniform J_l and $h_{\boldsymbol{r}}$) maps onto the uniform $D = 3$ Ising model. Thus, in this latter case, the *extremely disordered* system with annealed random exchange constants exhibits the standard $D = 3$ Ising-type behavior of uniform systems.

By the dualities of Secs. V A and V B, general multiparticle, or multispin, spatiotemporal correlation functions in different systems can be related to one another. In particular, by Eq. (28) relating the Majorana system with the QIG theory, the two

correlators

$$\left\langle \prod_{r,l} \mathcal{P}_r(t)(ic_{l1}c_{l2})(t') \right\rangle = \left\langle \prod_{r,l} \widetilde{\mathcal{P}}_r(t)\sigma_l^x(t') \right\rangle \quad (66)$$

are equal. Thus, if certain correlators (e.g., standard static two-point correlation functions, autocorrelation functions, or four-point correlators such as those prevalent in the study of glassy systems)[45] appear in the spin systems, then dual correlators appear in the interacting Majorana system with identical behavior. An exact duality preserves the equations of motion, and so the dynamics of dual operators are the same.[31] Similarly, by the duality of Eq. (35), the phase diagrams describing the Majorana networks are identical to those of QIG systems. In instances in which the QIG theories have been investigated, the phase boundaries in the Majorana system may thus be mapped out without further ado.

Lattice gauge theories with homogeneous couplings, i.e., uniform lattices, have been investigated extensively.[42,46] As we alluded to above, it is well appreciated that the QIG theory on a square lattice can be related, via a Feynman mapping, to an Ising gauge theory on the cubic lattice with the classical action

$$\mathcal{S}_{\text{IG}} = -K \sum_P \mathcal{P}_P. \quad (67)$$

The latter has a transition[47] at $K = K_c = 0.761\,423$, a value dual[46] to the critical coupling (or inverse critical temperature when the exchange constant is set to unity) of the $D = 3$ classical Ising model with nearest-neighbor coupling $\tilde{K}_c = 0.221\,659\,5$. Similar transitions between a confined (small K) to a deconfined (large K) phase appear in general uniform coupling lattice gauge theories with other geometries. Phase transitions mark singularities of the free energy, which are always identical in any two dual models.[31] In our case of interest here, by the correspondence of Eq. (35), identical transition points must thus appear in the dual Majorana theories. In particular, the transition points in the Majorana system are immediately determined by their dual-spin counterpart. More precisely, the Majorana uniform network depicted in Fig. 1 displays a quantum critical point of the $D = 3$ Ising universality class at $(J/h)_c = -2\tilde{K}_c/\ln\tanh\tilde{K}_c = 0.29112$.

In theories with sufficient disorder (e.g., quenched exchange couplings, fields, or spatially varying coordination number), rich behavior such as that exemplified by spin-glass transitions or Griffiths singularities[48] may appear. According to Eq. (35), in architectures with nonequidistant superconducting grains of random sizes, the effective couplings $\{J_l\}$ and $\{h_r\}$ are not uniform and may lead to spin glass, Griffiths, or other behavior whenever the corresponding dual gauge theory exhibits these as well. We note that the random transverse-field Ising model of Eq. (65) is well known to exhibit a (quantum) spin-glass behavior.[49,50] If and when it occurs, glassy (or spin-glass) dynamics in the annealed or gauge spin systems will, by our mapping, imply corresponding glassy (or spin-glass) dynamics in the Majorana system as well as interacting electronic systems (leading to *electron-glass* behavior). The disordered quantum Ising model was employed in the study of the insulator to superconducting phase transition in granular

superconductors.[51] Numerous electronic systems are indeed nonuniform[52] and/or disordered.[53]

VI. SPIN DUALS TO SQUARE LATTICE MAJORANA SYSTEMS

Thus far, we provided a systematic analysis of symmetries and dualities for Majorana systems supported on networks in any number of spatial dimensions. It is instructive to consider particularly simple architectures as these highlight salient features and, on their own merit, provide new connections among well-studied theories. In what follows, we will focus on the square lattice superconducting grain array of Fig. 1, and some honeycomb and checkerboard lattice spin-dual models.

A. XXZ honeycomb compass model

The Majorana system H_M of Eq. (5) in a square lattice is dual to a very interesting spin Hamiltonian on the honeycomb lattice (see Fig. 8). The dual-spin model may be viewed as an intermediate between the classical Ising model on the honeycomb lattice [involving products of a single spin component (σ^z) between nearest neighbors] and Kitaev's honeycomb model,[18] for which the bonds along the three different directions in the lattice are, respectively, pairwise products of the three different spin components. This particular spin Hamiltonian, which we dub *XXZ honeycomb compass model*, is described by

$$H_{\text{XXZh}} = -\sum_{\text{nonvertical links}} J_l\, \sigma_r^x \sigma_{r+\hat{e}_l}^x - \sum_{\text{vertical links}} h_r\, \sigma_r^z \sigma_{r+\hat{e}_z}^z,$$

$$(68)$$

where each $S = 1/2$ is located on the vertices r of a honeycomb lattice, and $\sigma_r^{x,z}$ are the corresponding Pauli matrices. The qualifier "nonvertical links" alludes to the two diagonally oriented directions of the honeycomb lattice, while "vertical links" are, as their name suggests, the links parallel to the vertical direction in Fig. 8. The unit vector $\hat{e}_l$ points along the diagonal link l and may be oriented along any of the two diagonal directions. The XXZ honeycomb compass model exhibits local symmetries associated with every lattice
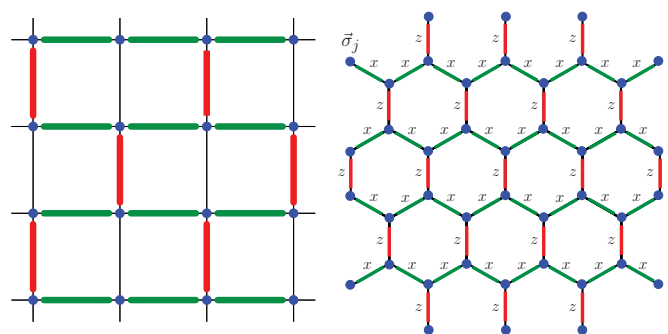

FIG. 8. (Color online) The brick-wall planar orbital compass model (Ref. 31) (shown on the left) can be seen as a simpler relative of the XXZ honeycomb compass model, by placing it on a honeycomb lattice as shown on the right.

site $\boldsymbol{r}$,

$$G_{\boldsymbol{r}}^{\text{XXZh}} = \sigma_{\boldsymbol{r}}^x \sigma_{\boldsymbol{r}+\hat{e}_z}^x. \tag{69}$$

Similarly, the XXZ system exhibits $d = 1$ symmetries of the form

$$Q_\ell^{\text{XXZh}} = \prod_{\boldsymbol{r}\in\ell} \sigma_{\boldsymbol{r}}^z \tag{70}$$

associated with every nonvertical contour ℓ (i.e., that composed of the diagonal nonvertical links) that circumscribes one of the toric cycles.

We provide, in the left-hand panel of Fig. 8, a simple schematic of the topology of the honeycomb lattice: that of a "brick-wall lattice."[29,54] The brick-wall lattice also captures the connections in the honeycomb lattice. It is formed by the union of the highlighted vertical (red) and horizontal (green) links in the left-hand side Fig. 8. The brick-wall lattice can be obtained by "squashing" the honeycomb lattice to flatten its diagonal links while leaving its topology unchanged in the process. In the brick-wall lattice, $\hat{e}_l$ simply becomes a unit vector along the horizontal direction. As can be seen by examining either of the panels of Fig. 8, the centers of the vertical links of the honeycomb (or brick-wall) lattice form, up to innocuous dilation factors, a square lattice. As is further evident on inspecting Fig. 8, between any pair of centers of neighboring vertical (red) links, there lies a center of a nondiagonal (green) link. This topological connection underlies the duality between the Majorana model on the square lattice and the XXZ honeycomb compass spin model. We explicitly classify the bonds in the Hamiltonian of Eq. (68) related to the two types of geometric objects:

(1) Bonds of type (i) are associated with the products $\{\sigma_{\boldsymbol{r}}^x \sigma_{\boldsymbol{r}+\hat{e}_l}^x\}$ on diagonal links of the lattice. They each anticommute with two.

(2) Bonds of type (ii), affiliated with products $\{\sigma_{\boldsymbol{r}}^z \sigma_{\boldsymbol{r}+\hat{e}_z}^z\}$ on the vertical links. Each one of these bonds anticommute with four bonds of type (i).

We merely note that replacing the bonds of the Majorana model on a square lattice, as they appear in the bond-algebraic relations (1–3) of Sec. V, by those above leads to three equivalent relations that completely specify the bond algebra of the system of Eq. (68). As we have earlier seen also the QIG theory of Eq. (27) and the annealed transverse-field Ising model of Eq. (48) have bonds that share the same three basic bond algebraic relations. Thus, we conclude that the XXZ honeycomb compass model is exactly dual to the QIG theory of Eq. (27) on the square lattice. In its uniform rendition (with all couplings J_l and fields $h_{\boldsymbol{r}}$ being spatially uniform), *the XXZ honeycomb compass system lies in the 3D Ising universality class.* Similarly, many other properties of the XXZ honeycomb compass model can be inferred from the heavily investigated QIG theory.

The duality between the XXZ honeycomb compass model and its Majorana system equal on the square lattice affords an example of a duality in which the Hilbert space size is preserved as we now elaborate. The XXZ theory of Eq. (68) is defined on a Hilbert space of size $\dim \mathcal{H}_{\text{XXZh}} = 2^{N_{\text{hl}}}$, where N_{hl} is the number of sites on the honeycomb lattice while that of the Majorana model of Eq. (5) was on a Hilbert space of dimension $\dim \mathcal{H}_{\text{M}} = 4^{N_{\boldsymbol{r}}}$. Now, for a given number $N_{\boldsymbol{r}}$

of vertical links on the honeycomb lattice, we have the same number of bonds of types (i) and (ii) as we had in the Majorana system while having $N_{\text{hl}} = 2N_{\boldsymbol{r}}$ lattice sites.

B. Checkerboard model of $(p + ip)$ superconducting grains

In Ref. 55, Xu and Moore, motivated by an earlier work of Moore and Lee,[56] proposed the following spin Hamiltonian,

$$H_{\text{XM}} = -\sum_{\boldsymbol{r}} \left(h_{\boldsymbol{r}}^{\text{XM}} \sigma_{\boldsymbol{r}}^x + J_\square^{\text{XM}} \square \sigma_{\boldsymbol{r}}^z \right), \tag{71}$$

to describe the time-reversal symmetry-breaking characteristics in a matrix of unconventional p-wave granular superconductors on a square lattice. In writing Eq. (71), we employ a shorthand

$$\square \sigma_{\boldsymbol{r}}^z \equiv \sigma_{\boldsymbol{r}}^z \sigma_{\boldsymbol{r}+\boldsymbol{e}_1}^z \sigma_{\boldsymbol{r}+\boldsymbol{e}_1+\boldsymbol{e}_2}^z \sigma_{\boldsymbol{r}+\boldsymbol{e}_2}^z \tag{72}$$

to denote the square lattice plaquette product, where $\boldsymbol{e}_1$ and $\boldsymbol{e}_2$ denote unit vectors along the principal lattice directions. For the benefit of the astute reader, we remark that this open square notation for the *product* should not be confused with our general notation for the elementary plaquette loops P that we use throughout this work. It is important to emphasize that the spins $\sigma_{\boldsymbol{r}}^{x,z}$ in Eqs. (71) and (72) are situated at the vertices $\boldsymbol{r}$ of the square lattice [not on the links (or link centers) as in gauge theories]. The eigenvalues $\sigma_{\boldsymbol{r}}^z = \pm 1$ describe whether the superconducting grain located at the vertex of the square lattice $\boldsymbol{r}$ has a $(p + ip)$ or a $(p - ip)$ order parameter.

We show next that a $D = 2$ *checkerboard* rendition of the XM model which we denote by CXM (see Fig. 9) is dual to the Majorana system on the square lattice (which is, as we showed, dual to the XXZ honeycomb compass model and all of the other models that we discussed earlier in this work). This system is defined by the following Hamiltonian:

$$H_{\text{CXM}} = -\sum_{\boldsymbol{r}} h_{\boldsymbol{r}} \sigma_{\boldsymbol{r}}^x - \sum_{x_1+x_2=\text{odd}} J_\square^{\text{XM}} \square \sigma_{\boldsymbol{r}}^z. \tag{73}$$
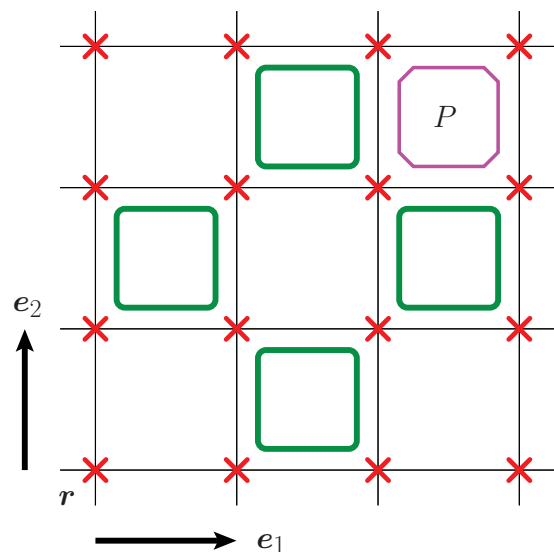

FIG. 9. (Color online) The checkerboard Xu-Moore (CXM) model of Eq. (73). The symmetry plaquettes P constitute half of all the plaquettes of the lattice, while the interaction plaquettes $\square \sigma_{\boldsymbol{r}}^z$ represent the other half.

In this system, the plaquette operators $\Box \sigma_r^z$ (with $r = x_1 e_1 + x_2 e_2$) appear in every other plaquette (hence the name "checkerboard"). These plaquettes are present only if $x_1 + x_2$ is an odd integer as emphasized in Eq. (73). The model has the following local symmetries:

$$G_P = \prod_{r \in P} \sigma_r^x, \qquad (74)$$

where P are those plaquettes appearing whenever $x_1 + x_2$ is an even integer.

The proof of our assertion above concerning the duality of this system to the Majorana system of Eq. (5) when implemented on the square lattice is straightforward and will mirror, once again, all of our earlier steps. We may view the Hamiltonian of Eq. (73) as comprised of two basic types of bonds:

(1) Bonds of type (i) are onsite operators $\{\sigma_r^x\}$ associated with local transverse fields.

(2) Bonds of type (ii) are the plaquette product operators $\{\Box \sigma_r^z\}$ of Eq. (72), for plaquettes, the bottom left-hand corner r of which is an "odd" site.

The basic network structure underlying these bonds is simple and, apart from an interchange of names, identical to that of the Majorana system on the square lattice of Fig. 1 as well as that of the XXZ honeycomb compass model of Fig. 8. To see this, we note that in the checkerboard of Fig. 9, the fourfold-coordinated interaction plaquettes generate, on their own, a square lattice grid. Between any two neighboring interaction plaquettes on this square lattice array, there is a lattice site r (see Fig. 10). As in our earlier proof of the duality, we simply remark that replacing the bonds of the Majorana model on a square lattice, as they appear in the bond-algebraic relations (1–3) of Sec. V, by those above leads to three equivalent relations that completely specify the bond algebra of the CXM system. The Majorana and CXM models are thus dual to one another ($H_M \leftrightarrow H_{CXM}$) when their couplings are related via the correspondence

$$\begin{aligned} J_l &\leftrightarrow h_r^{XM}, \\ h_r &\leftrightarrow J_{\Box}^{XM}. \end{aligned} \qquad (75)$$

Thus, the CXM model joins the fellowship of all other dual theories (with the same network connectivity) that we
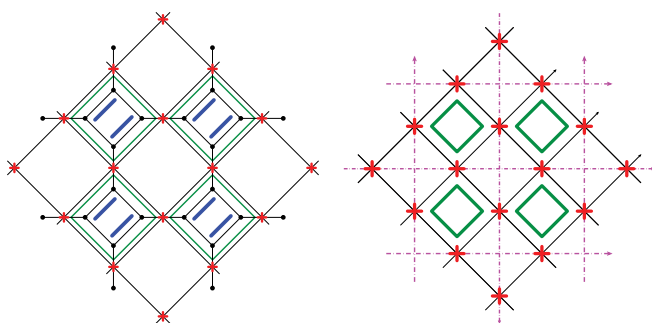

FIG. 10. (Color online) The $D = 2$ checkerboard Xu-Moore (CXM) model is dual to the Majorana system in a square lattice as shown on the left. On the right, we rotate and redefine the lattice in a manner which highlights its connection to the QIG theory of Eq. (27).

discussed in this work (i.e., the Majorana, QIG, and annealed transverse-field Ising models on the square lattice as well as the XXZ compass model on the honeycomb (or equivalent brick-wall) lattice).

On the right-hand half of Fig. 10, we pictorially illustrate the connection between the CXM model and the QIG theory. The individual sites of the checkerboard lattice of Fig. 9 (the sites at which the local transverse fields are present) map onto links of the gauge theory (Sec. V A). Similarly, the interaction plaquettes of the CXM model map into plaquettes of the QIG theory. Note, on the right, that as is geometrically well appreciated, the four center points of the individual links on the square (gauge theory) lattice can either circumscribe interaction plaquettes of the gauge theory or may correspond to four links that share a common endpoint that do form a "star" configuration.[31] In particular, by its duality to the QIG theory, the CXM rigorously lies in the 3D Ising universality class when the couplings $J_{\Box}^{XM}$ and h_r^{XM} are spatially uniform. For a given equal number of bonds in both the Majorana system and the CXM theory, it is readily seen that the Hilbert space dimensions of both theories are the same, $\dim \mathcal{H}_M = \dim \mathcal{H}_{CXM}$.

VII. QUANTUM SIMULATIONS WITH MAJORANA NETWORKS

The Dirac, fermionic, annihilation and creation operators $\{d_r\}$ and $\{d_r^\dagger\}$, respectively, can be expressed as a linear combination of two Majorana fermion operators. For example, if we are interested in *two-flavor* Dirac operators, a possible realization is (see Fig. 1)

$$\begin{aligned} d_{r\uparrow} &= \frac{1}{\sqrt{2}}(c_{l_1 1} + i c_{l_3 2}), \quad d_{r\uparrow}^\dagger = \frac{1}{\sqrt{2}}(c_{l_1 1} - i c_{l_3 2}), \\ d_{r\downarrow} &= \frac{1}{\sqrt{2}}(c_{l_2 1} + i c_{l_4 2}), \quad d_{r\downarrow}^\dagger = \frac{1}{\sqrt{2}}(c_{l_2 1} - i c_{l_4 2}), \end{aligned} \qquad (76)$$

where $r \in l_1, l_2, l_3, l_4$.

A system of interacting Dirac fermions (e.g., electrons) on a general graph can be mapped onto that of twice the number of Majorana fermions on the same graph, and each Dirac fermion is to be replaced by two Majorana fermions following the substitution of Eq. (76). Thus, any granular system of the form of Eq. (5) in which each grain r has $q_r = 2z_r$ neighbors can be mapped onto a Dirac fermionic system on the same graph in which on each grain there are z_r Dirac fermions. There are many possible ways to pair up the Majorana fermions in the system of Eq. (5) to yield a corresponding system of Dirac fermions. Equation (76) represents just one possibility. Another possible way to generate (spinless) Dirac fermions is

$$d_l = \frac{1}{\sqrt{2}}(c_{l1} + i c_{l2}), \quad d_l^\dagger = \frac{1}{\sqrt{2}}(c_{l1} - i c_{l2}). \qquad (77)$$

All of the spin duals that we derived for Majorana fermion systems hold, mutatis mutandis, for these systems of Dirac fermions on arbitrary graphs. In this sense, our dualities afford an alternative, flexible approach to fermionization that does not rely on the Jordan-Wigner transformation.[31] Most importantly, one can use these mappings to simulate models of strongly interacting Dirac fermions, such as Hubbard-type

models, on the experimentally realized Majorana networks. In other words, one can engineer *quantum simulators* out of these Josephson junction arrays.

As a concrete example, we consider the square lattice array of Fig. 1 and transform, on this lattice, the Majorana system of Eq. (5) into a *two-flavor Hubbard model with compass-type pairing and hopping*. Based on our analysis thus far, we will illustrate that this variant of the 2D Hubbard model is exactly dual to the 2D QIG theory and thus lies in the 3D Ising universality class. Consider the mapping of Eq. (76). With $n_{r\sigma} = d^\dagger_{r\sigma} d_{r\sigma}$ ($\sigma = \uparrow, \downarrow$), a Hubbard-type term with onsite repulsion U_r becomes

$$U_r(n_{r\uparrow} - 1)(n_{r\downarrow} - 1) = U_r(\mathcal{P}_r - 1), \qquad (78)$$

akin to the second term of Eq. (5) with $h_r \leftrightarrow U_r$ (up to an irrelevant constant). In what follows, we assume that the network array of Fig. 1 has unit lattice constant.

The Majorana bilinear that couples, for instance, the bottom-most corner of the grain that is directly above r (i.e., site $r + e_2$) to the top-most site of grain r (with thus a link l that is vertical) becomes

$$-i J_l c_{l_21} c_{l_22} = \frac{J_l}{2}(d^\dagger_{r\downarrow} + d_{r\downarrow})(d^\dagger_{r+e_2\downarrow} - d_{r+e_2\downarrow}). \qquad (79)$$

Similarly, for horizontal links l, the bilinear in the first term of Eq. (5) realizes pairing hopping terms involving only the $\uparrow$ flavor of the fermions. Thus, the Hamiltonian of Eq. (5) becomes a Hubbard-type Hamiltonian with bilinear terms containing hopping and pairing terms between electrons of the up or down flavor for links l that are vertical or horizontal, respectively. Such a dependence of the interactions between the internal spin flavor on the relative orientation of the two interacting electrons in real space bears a resemblance to "compass-type" systems.[57] Putting all our results together, the Dirac fermion Hamiltonian on the square lattice with pair terms of the form of Eq. (79) augmented by the onsite Hubbard-type interaction term of Eq. (78) is dual to all of the other models that we considered thus far in this work. In particular, as such this interacting Dirac fermion (or electronic) system *is not of the canonical noninteracting Fermi liquid form*. Rather, this system lies in the 3D Ising universality class.

The standard Hubbard model with SU(2) spin symmetry, which up to chemical potential terms is given by ($\alpha = 1,2$)

$$H_{\text{Hub}} = -t \sum_{r,\alpha,\sigma} (d^\dagger_{r\sigma} d_{r+e_\alpha\sigma} + \text{H.c.})$$
$$+ U \sum_r (n_{r\uparrow} - 1)(n_{r\downarrow} - 1), \qquad (80)$$

can be written as a sum of terms of the form of Eq. (78) augmenting many Majorana fermion bilinear coupling sites on nearest-neighbor grains (i.e., r and $r \pm e_\alpha$). As we illustrate in Fig. 11, we label the four Majorana modes on each grain r as $\{c_{ra}\}^4_{a=1}$. In terms of these, the Hubbard Hamiltonian becomes

$$H_{\text{Hub}} = -t \sum_{r,\alpha,a=1,2} i(c_{ra} c_{r+e_\alpha a+2} + c_{r+e_\alpha a} c_{ra+2})$$
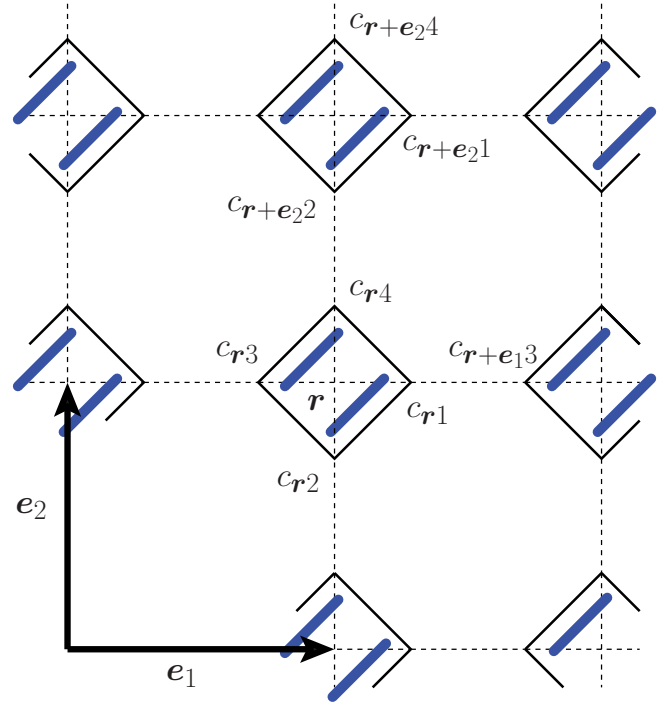$$+ U \sum_r (\mathcal{P}_r - 1). \qquad (81)$$

FIG. 11. (Color online) A labeling of the Majorana wire endpoints on the square lattice which we use here to explicitly represent the standard electronic Hubbard model in terms of Majorana operators. This is a different labeling than the one in Fig. 1.

Thus, the Hubbard Hamiltonian may be simulated via Majorana wires with multiple Josephson junctions. Appendix A describes the possible simulation of the transverse-field Ising chain via Majorana networks.

VIII. CONCLUSIONS

We conclude with a brief synopsis of our findings. This work focused on the interacting Majorana systems of Eq. (5) *on general lattices and networks*. Aside from fundamental questions in particle physics and viable realizations as emergent excitations in condensed matter physics, as we have further discussed in this paper, Majorana systems may hold promise for simulations and quantum information. By employing the standard representation of Dirac fermions as a linear combination of Majorana fermions, our results similarly hold for a general class of interacting Dirac fermion systems on general graphs. Towards this end, we heavily invoked two principal tools: (i) The use of d-dimensional gaugelike symmetries that mandate dimensional reduction and TQO via correlation function bounds.[26,33,37] These symmetries lead to bounds on the autocorrelation times.[26] (ii) The bond-algebraic theory of dualities[26–32] as it, in particular, pertains to very general dualities and fermionization[30,31] to obtain multiple exact spin duals to these systems, in arbitrary dimensions and boundary conditions, and for finite or infinite systems. Using these approaches, we arrived at general dimensional fermionization and demonstrated the following:

(i) The Majorana systems of Eq. (5), standard QIG theories Eq. (27), and transverse-field Ising models with annealed bimodal disorder Eq. (48) are all dual to one another on general

lattices and networks. The duality afforded an interesting connection between heavily disordered annealed Ising systems and uniform Ising theories. The spin duals further enable us to suggest and predict various transitions as well as spin-glass-type behavior in general interacting Majorana fermion (and Dirac fermion) systems. The representation of Dirac fermions via Majorana fermions enlarges the scope of our results. In particular, as Eq. (78) makes evident, the standard onsite Hubbard term in electronic systems is exactly of the same form as that of the intragrain coupling in the interacting Majorana systems that we investigated. We similarly represented the bilinear in the Majorana model of Eq. (5) as a Dirac fermion form Eq. (79). Following our dualities, on the square lattice, the interacting Dirac fermion (or electronic) Hamiltonian formed by the sum of all terms of the form of Eqs. (78) and (79) is dual to the QIG theory and thus lies in the 3D Ising universality class, notably different from standard noninteracting Fermi liquids; this nontrivial electronic system features Hubbard onsite repulsion augmented by "compass"-type hopping and pairing terms. We further showed how to quantum simulate bona fide Hubbard-type electronic Hamiltonians via Majorana wire networks.

(ii) Several systems were further introduced and investigated via the use of bond algebras: (1) the "XXZ honeycomb compass" model of Eq. (68) (a model intermediate between the classical Ising model on the honeycomb lattice and Kitaev's honeycomb model) and (2) a checkerboard version of the Xu-Moore model for superconducting $(p + ip)$ arrays Eq. (73). By the use of dualities, we illustrated that both of these systems lie in the 3D Ising universality class.

As evident in our work, the "computations" necessary to attain these results were, to say the least, very simple by comparison to other approaches to duality (and specifically those relating to attempts to arrive at a useful high-dimensional fermionization) that generally require far more involved calculations. In the Appendixes, we discuss other connections between Majorana and spin systems including Majorana simulators.

ACKNOWLEDGMENT

APPENDIX A: DUALITIES IN FINITE SYSTEMS WITH OPEN BOUNDARY CONDITIONS

We have, so far, studied *exact* dualities for the Majorana system with the Hamiltonian H_M of Eq. (5) when subject to periodic boundary conditions. We focused on periodic boundary conditions that are pertinent to the theoretical study of TQO. In this appendix, we will consider *exact* dualities in the presence of *open* boundary conditions. In doing so, we will further study finite, even quite small, square lattices. It is useful to provide a precise description of these finite dual-spin systems as there is a definite possibility that this Majorana architecture may become realizable in the next few years. These dualities also allow us to illustrate the flexibility of the bond-algebraic approach to dualities in handling a variety of boundary conditions *exactly*. As in the rest of this paper, the
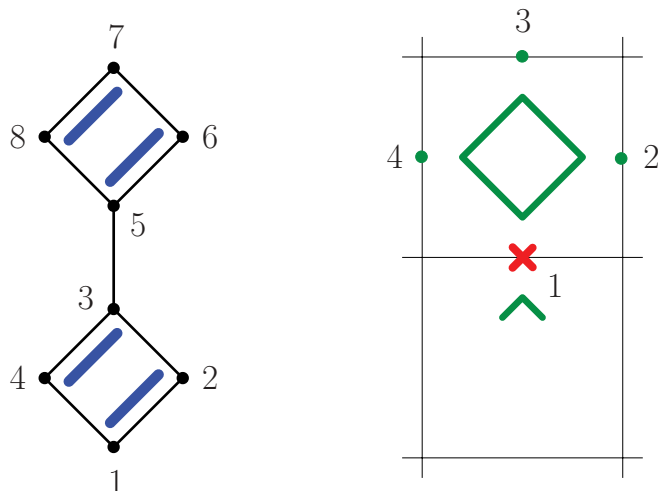

FIG. 12. (Color online) The spin dual of two superconducting islands. Each island maps to a plaquette interaction of the QIG theory, but such a mapping would not be compatible with matching dimensions of Hilbert spaces. Hence, one of the lower plaquettes is chopped to include only one spin.

dualities we obtain are exact unitary equivalences. Thus, these dualities may be tested numerically by checking if the energy spectra of the two dual systems are indeed identical.

As illustrated in Sec. V A, the effective Hamiltonian H_M on the square lattice and in the bulk is dual to the $\mathbb{Z}_2$ QIG theory. In this appendix, our task is to find the boundary terms that make the duality exact in the presence of open boundary conditions. Here, we only consider dualities that preserve the dimension of the Hilbert space of the two theories. We thus follow two guiding principles: (1) in the bulk, the dual-spin theory remains the $\mathbb{Z}_2$ QIG theory, and (2) on the boundary, we introduce terms that preserve both the bond algebra and the dimension of the Hilbert space. Let us start with the simplest interacting case, that of two islands (grains) linked by one Josephson coupling (see Fig. 12). In this case, the Hamiltonian of Eq. (5) reads as

$$H_M = -hc_1c_2c_3c_4 - h'c_5c_6c_7c_8 - Jic_3c_5. \qquad (A1)$$

This Hamiltonian acts on a Hilbert space of dimension $\dim \mathcal{H}_M = 2^{8/2} = 2^4$. Thus, the dual theory must contain four
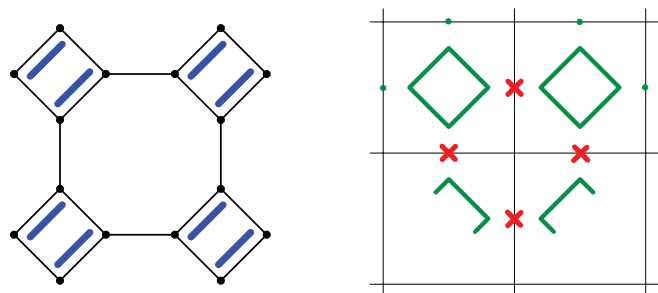

FIG. 13. (Color online) The spin dual for a configuration of four islands. The incomplete plaquettes represent two-spin interactions in the Hamiltonian.
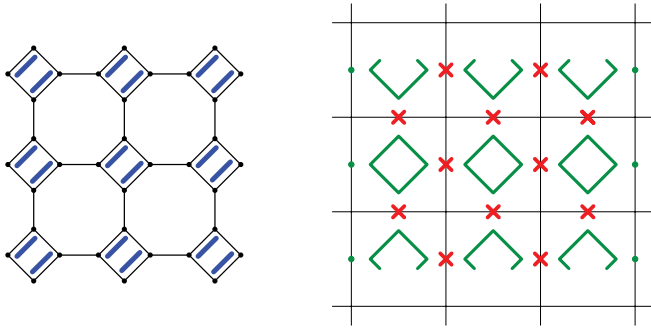
FIG. 14. (Color online) The spin dual for nine islands. Incomplete plaquettes represent three-spin interactions in the spin Hamiltonian, the product of the three spins σ^z closer to an incomplete green diamond.

spins and some recognizable gauge interactions. The result is

$$H_{\text{QIG}} = -h\sigma_1^z - h'\sigma_1^z\sigma_2^z\sigma_3^z\sigma_4^z - J\sigma_1^x, \tag{A2}$$

where the single spin σ_1^z in the Hamiltonian stands for an *incomplete plaquette*. One can check that the bond algebra is preserved and the two spectra are identical.

The next interesting case contains four superconducting islands (see Fig. 13). In this case, dim $\mathcal{H}_{\text{M}} = 2^{16/2} = 2^8$, and so the dual-spin Hamiltonian, described diagrammatically in Fig. 13, contains eight spins, two complete and two incomplete gauge plaquettes. The situation becomes more regular if we further increase the number of islands. For 9 islands (dim $\mathcal{H}_{\text{M}} = 2^{36/2} = 2^{18}$), the Majorana system maps to 18 spins, 3 complete, and 6 incomplete plaquettes on the first and last rows of the spin model. One can generalize this picture to L^2 islands. Then, the dual $\mathbb{Z}_2$ QIG theory will be represented by a scaled version of the right panel of Fig. 14, with $2L^2$ spins, and $2L$ incomplete plaquettes (the product of only three spins σ^z). The latter incomplete plaquettes are equally split between the top and bottom rows, i.e., L incomplete plaquettes are placed on the top row and L are situated on the bottom row.

Notice that there is no natural guiding principle to find the dual theory by a Jordan-Wigner mapping. The bond-algebraic method is the natural approach and can be tested numerically on finite lattices.

APPENDIX B: FERMIONIZATION OF $S = 1/2$ SPIN MODELS IN ARBITRARY DIMENSIONS

Although not pertinent to our direct models of study [those of Eq. (5) and their exact duals], we briefly review and discuss, for the sake of completeness and general perspective, dualities of related quantum spin $S = 1/2$ systems. General bilinear spin Hamiltonians can be expressed as a quartic form in Majorana fermion operators. The general nature of this mapping is well known and has been applied to other spin systems with several twists. Simply put, we can write each spin operator as a quadratic form in Majorana fermions. In the case of general *two-component* spin systems that we discuss now, the relevant Pauli algebra is given by the following onsite ($\boldsymbol{r}$) constraints:

$$\left(\sigma_{\boldsymbol{r}}^x\right)^2 = \left(\sigma_{\boldsymbol{r}}^z\right)^2 = 1, \quad \{\sigma_{\boldsymbol{r}}^x, \sigma_{\boldsymbol{r}}^z\} = 0, \tag{B1}$$

and trivial off-site ($\boldsymbol{r} \neq \boldsymbol{r}'$) relations

$$\left[\sigma_{\boldsymbol{r}}^x, \sigma_{\boldsymbol{r}'}^z\right] = 0. \tag{B2}$$

A dual Majorana form may be easily derived as follows. We consider a dual Majorana system in which at each lattice site $\boldsymbol{r}$ there is a grain with three relevant Majorana modes. We label the three relevant Majorana modes (out of any larger number of modes on each grain) by $\{c_{\boldsymbol{r},a}\}_{a=1}^3$. As can be readily seen by invoking Eq. (4), a representation that trivially preserves the algebraic relations of Eqs. (B1) and (B2) is given by

$$\sigma_{\boldsymbol{r}}^x \leftrightarrow ic_{\boldsymbol{r}1}c_{\boldsymbol{r}2}, \quad \sigma_{\boldsymbol{r}}^z \leftrightarrow ic_{\boldsymbol{r}1}c_{\boldsymbol{r}3}. \tag{B3}$$

Equation (B3) is a variant of a well-known mapping applicable to three component spins (as well as, trivially, spins with any smaller number of components).[12,58] Equation (B3) may also be viewed as a two-component version of the mapping employed by Kitaev.[18] The Hilbert space spanned by an $S = 1/2$ spin system on a lattice/network having N sites is dim $\mathcal{H}_{\text{spin}} = 2^N$. By contrast, the Hilbert space of a general Majorana system with $\{m_{\boldsymbol{r}}\}$ Majorana modes ($m_{\boldsymbol{r}} \geqslant 3$) at sites $\{\boldsymbol{r}\}$ is given by dim $\mathcal{H}_{\text{M}} = 2^{\sum_{\boldsymbol{r}} m_r/2}$. Thus, in this duality, the Hilbert space is not preserved: each individual energy level of the spin system becomes ($2^{(\sum_{\boldsymbol{r}} m_r/2)-N}$)-fold degenerate. Similarly, one-component systems (e.g., those involving only $\{\sigma_{\boldsymbol{r}}^x\}$) can be mapped onto a granular system with two Majorana modes per site. If there are two Majorana modes at each site $\boldsymbol{r}$, then such a mapping will preserve the Hilbert space size.

For completeness, we now turn to specific spin systems related to those that we discussed in the main part of our article. In Sec. VI B, we illustrated that the Majorana system of Eq. (5) (and all of its duals that we earlier discussed in the text) can be mapped onto the Xu-Moore model[55] on the checkerboard lattice. Following our general discussion above, it is straightforward to provide a Majorana dual to the Xu-Moore model on the square lattice, Eq. (71). On the square lattice, the orbital compass model (OCM) and the Xu-Moore model of Eq. (71) are dual to one another.[30,31,59] We will assume the square lattice to define the xz plane. The anisotropic square lattice OCM (Refs. 57 and 59) is given by
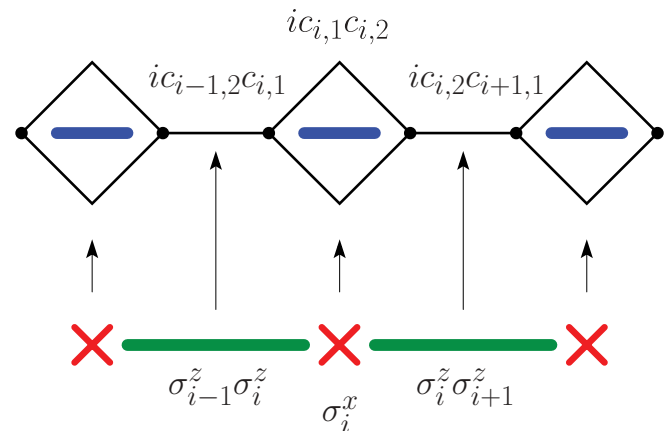

FIG. 15. (Color online) The transverse-field Ising model can be simulated by an architecture of nanowires with one wire per superconducting island.

the Hamiltonian

$$H_{\text{OCM}} = -\sum_{r} \left(J_{x;r} \sigma_r^x \sigma_{r+e_1}^x + J_{z;r} \sigma_r^z \sigma_{r+e_2}^z \right). \quad \text{(B4)}$$

In Eq. (B4), we generalized the usual compass model Hamiltonian by allowing the couplings $\{J_{x,z}\}$ to vary locally with the location of the horizontal and vertical links of the square lattice [given by $(r, r + e_{1,2})$ respectively]. By plugging Eqs. (B3) into (B4), we can rewrite this (as well as other general two-component spin bilinears) as a quartic form in the Majorana fermions.

APPENDIX C: QUANTUM SIMULATION OF THE TRANSVERSE-FIELD ISING CHAIN

It may generally be feasible to use our formalism to simulate quantum-spin models in terms of Majorana networks. Consider, for example, the simulation of a transverse-field Ising chain

$$H_{\text{I}} = -\sum_{i=1}^{N-1} J_i \sigma_i^z \sigma_{i+1}^z - \sum_{i=1}^{N} h_i \sigma_i^x \quad \text{(C1)}$$

with N spins and open boundary conditions. In this case, it may be possible to use linear arrays with one nanowire per island to simulate this model and study, for instance, the dynamics of its quantum phase transition. The Hamiltonian H_{I} maps to the Majorana network

$$H_{\text{M}} = -i \sum_{i=1}^{N-1} J_i c_{i,2} c_{i+1,1} - i \sum_{i=1}^{N} h_i c_{i,1} c_{i,2}, \quad \text{(C2)}$$

after the following duality mapping:

$$\sigma_i^z \sigma_{i+1}^z \mapsto i c_{i,2} c_{i+1,1}, \quad \sigma_i^x \mapsto i c_{i,1} c_{i,2} \quad \text{(C3)}$$

(see Fig. 15).

---

[1] E. Majorana, Nuovo Cimento **14**, 171 (1937).

[2] C. W. J. Beenakker, Annual Review of Condensed Matter Physics **4** (2013).

[3] F. Wilczek, Nat. Phys. **5**, 614 (2009).

[4] M. Franz, Physics **3**, 24 (2010).

[5] J. Alicea, Phys. Rev. B **81**, 125318 (2010).

[6] L. Fu and C. L. Kane, Phys. Rev. Lett. **100**, 096407 (2008).

[7] J. Nilsson, A. R. Akhmerov, and C. W. J. Beenakker, Phys. Rev. Lett. **101**, 120403 (2008).

[8] A. Yu. Kitaev, Phys.-Usp. **44**, 131 (2001).

[9] J. D. Sau, R. M. Lutchyn, S. Tewari, and S. Das Sarma, Phys. Rev. Lett. **104**, 040502 (2010).

[10] R. M. Lutchyn, J. D. Sau, and S. Das Sarma, Phys. Rev. Lett. **105**, 077001 (2010).

[11] Y. Oreg, G. Refael, and F. von Oppen, Phys. Rev. Lett. **105**, 177002 (2010).

[12] R. R. Biswas, C. R. Laumann, and S. Sachdev, Phys. Rev. B **84**, 235148 (2011).

[13] H. H. Lai and O. I. Motrunich, Phys. Rev. B **84**, 235148 (2011).

[14] D. A. Ivanov, Phys. Rev. Lett. **86**, 268 (2001).

[15] N. Read and D. Green, Phys. Rev. B **61**, 10267 (2000).

[16] S. Deng, L. Viola, and G. Ortiz, Phys. Rev. Lett. **108**, 036803 (2012).

[17] L. Fu, Phys. Rev. Lett. **104**, 056402 (2010).

[18] A. Kitaev, Ann. Phys. (NY) **321**, 2 (2006).

[19] C. Xu and L. Fu, Phys. Rev. B **81**, 134435 (2010).

[20] B. M. Terhal, F. Hassler, and D. P. DiVincenzo, Phys. Rev. Lett. **108**, 260504 (2012).

[21] A. Kitaev, Ann. Phys. (NY) **303**, 2 (2003).

[22] C. Nayak, C. Simon, C. A. Stern, M. Freedman, and S. Das Sarma, Rev. Mod. Phys. **80**, 1083 (2008).

[23] E. Lieb, T. Schultz, and D. Mattis, Ann. Phys. (NY) **16**, 407 (1961).

[24] S. Nadj-Perge, V. S. Pribiag, J. W. G. van den Berg, K. Zuo, S. R. Plissard, E. P. A. M. Bakkers, S. M. Frolov, and L. P. Kouwenhoven, Phys. Rev. Lett. **108**, 166801 (2012).

[25] E. Fradkin, M. Srednicki, and L. Susskind, Phys. Rev. D **21**, 2885 (1980).

[26] Z. Nussinov, G. Ortiz, and E. Cobanera, arXiv:1110.2179, Annals of Physics, to appear (2012).

[27] Z. Nussinov and G. Ortiz, Phys. Rev. B **77**, 064302 (2008).

[28] Z. Nussinov and G. Ortiz, Phys. Rev. B **79**, 214440 (2009).

[29] Z. Nussinov and G. Ortiz, Europhys. Lett. **84**, 36005 (2008).

[30] E. Cobanera, G. Ortiz, and Z. Nussinov, Phys. Rev. Lett. **104**, 020402 (2010).

[31] E. Cobanera, G. Ortiz, and Z. Nussinov, Adv. Phys. **60**, 679 (2011).

[32] G. Ortiz, E. Cobanera, and Z. Nussinov, Nucl. Phys. B **854**, 780 (2011).

[33] Z. Nussinov and G. Ortiz, Ann. Phys. (NY) **324**, 977 (2009); Proc. Natl. Acad. Sci. USA **106**, 16944 (2009).

[34] On each grain, the z_r nonintersecting nanowires link one half of the nanowire endpoints to the remaining half; there are $(2z_r)!/(2^{z_r} z_r!)$ distinct ways for different pairings of the vertices. These nonintersecting nanowires can be placed in any way on a surface of the bulk superconducting grain. For instance, in the square and triangular lattices, the regular arrangement of nanowires shown in Figs. 1 and 3 is only one among many others.

[35] It us useful at this point to recall some basic algebraic facts about Majorana fermions. Let us label the Majorana operators simply as $c_i, i = 1, \ldots, N$. Then,

$$\{c_i, c_j\} = 2\delta_{i,j}, c_i^\dagger = c_i.$$

In general, the square of the string product of Majorana operators,

$$(c_1 \ldots c_N)^2 = (-1)^{N(N-1)/2} \mathbb{1},$$

so that the eigenvalues of $c_1 \ldots c_N$ are ± 1 or $\pm i$, depending on N. If N is even, up to equivalence, there is only one irreducible representation (irrep) for these relations. It acts on a Hilbert space of dimension $\dim \mathcal{H}_{\text{M}}(N \text{even}) = 2^{N/2}$, and can be described in terms of Pauli matrices as

$$c_i = \begin{cases} \sigma_i^x (\sigma_{i-1}^z \ldots \sigma_1^z), & i = 1, \ldots, \frac{N}{2} \\ \sigma_{i-\frac{N}{2}}^y (\sigma_{i-\frac{N}{2}-1}^z \ldots \sigma_1^z), & i = 1 + \frac{N}{2}, \ldots, N. \end{cases}$$

If N is odd,

$$[c_1 \ldots c_N, c_i] = 0.$$

So, in view of the above relation concerning the square of the string product of Majorana operators, the irreps are characterized by an

extra constraint,

$$c_1 \ldots c_N = \alpha \mathbb{1} \quad \text{(irrep for } N \text{ odd)}$$

with $\alpha = \pm 1, \pm i$ depending on N and the particular irrep. An explicit irrep is afforded by

$$c_i = \begin{cases} \sigma_i^x \left(\sigma_{i-1}^z \ldots \sigma_1^z \right), & i = 1, \ldots, \frac{N-1}{2} \\ \sigma_{i-\frac{N-1}{2}}^y \left(\sigma_{i-\frac{N-1}{2}-1}^z \ldots \sigma_1^z \right), & i = \frac{N+1}{2}, \ldots, N-1 \\ \sigma_1^z \ldots \sigma_{\frac{N-1}{2}}^z, & i = N. \end{cases}$$

Its dimension is $\dim \mathcal{H}_M(N \text{odd}) = 2^{(N-1)/2}$.

[36] A definite order is to be assigned on each grain. As will become evident, an odd permutation of the ordering of the Majorana operators in the product of Eq. (6), which leads by virtue of the Majorana algebra to a sign change, will not change the *bond algebra* (to be defined later) and thus none of our dualities.

[37] C. D. Batista and Z. Nussinov, Phys. Rev. B **72**, 045137 (2005).

[38] In these and other general systems, not all $d = 1$ gaugelike symmetries are independent. If the Majorana system has a trivial homology (such as that of an infinite plane or a sphere), no $d = 1$ gaugelike symmetries appear: all symmetries involving $\mathcal{O}(L^1)$ sites can be expressed in terms of a product of the local symmetries and thus are not fundamental. By contrast, for a $D = 2$-dimensional system placed on a torus, there are two closed toric cycles ℓ independent of the local symmetries. This explains the findings of Ref. 20 that the Majorana theory has TQO without the need to apply perturbation theory. Some manifestations of this phenomenon were noticed in numerical simulations of compact QED (Ref. 60), although not recognized as a signal of the presence or absence of TQO. In numerous theories with plaquette and/or link interactions, the Euler-Lhuillier formula $V - E + F = 2(1 - g)$ relating the genus number g of the manifold on which the system is embedded to the number of local faces (F), edges (E), and vertices (V) affords us with a knowledge of the number of independent ($d = 1$) symmetry operators (loops around independent cycles) that the system may have that can not be written in terms of local operators. This and related aspects have been discussed elsewhere (Ref. 33).

[39] S. Elitzur, Phys. Rev. D **12**, 3978 (1975).

[40] R. L. Jack and L. Berthier, Phys. Rev. E **85**, 021120 (2012).

[41] We parenthetically remark that in the case of non-planar graphs (which we do not consider here), the three relations of Eqs. (24)–(26) are augmented by an additional constraint: (4) the product of all plaquette operators associated with plaquettes that completely tile any closed volume must be the identity operator. For instance, on a simple cubic lattice, the product of the six plaquette operators associated with the six faces of each elementary cube of the lattice (the minimal volume of the lattice from which all other closed volumes can be constructed) must equal the identity operator.

[42] E. Fradkin and L. Susskind, Phys. Rev. D **17**, 2637 (1978).

[43] The connection to the QIG theory claimed in Ref. [20] was made after we established it rigorously in the arXiv version of the present paper.

[44] J. B. Kogut, Rev. Mod. Phys. **51**, 659 (1979).

[45] N. Lacevic, F. W. Starr, T. B. Schroder, and S. C. Glotzer, J. Chem. Phys. **119**, 7372 (2003).

[46] F. J. Wegner, J. Math. Phys. **12**, 2259 (1971).

[47] C. Itzykson and K-M. Drouffe, in *Statistical Field Theory*, Vol. 1 (Cambridge University Press, Cambridge, 1989), p. 355.

[48] R. B. Griffiths, Phys. Rev. Lett. **23**, 17 (1969).

[49] D. S. Fisher, Phys. Rev. Lett. **69**, 534 (1992).

[50] M. Schechter, Phys. Rev. B **77**, 020401(R) (2008).

[51] L. B. Ioffe and M. Mezard, Phys. Rev. Lett. **105**, 037001 (2010); M. V. Feigelman, L. B. Ioffe, and M. Mezard, Phys. Rev. B **82**, 184534 (2010).

[52] M. B. Salamon and M. Jaime, Rev. Mod. Phys. **73**, 583 (2001); J. M. Tranquada, B. J. Sternlieb, J. D. Axe, Y. Nakamura, and S. Uchida, Nature (London) **375**, 561 (1995); M. P. Lilly, K. B. Cooper, J. P. Eisenstein, L. N. Pfeiffer, and K. W. West, Phys. Rev. Lett. **82**, 394 (1999).

[53] S. Bogdanovich and D. Popovic, Phys. Rev. Lett. **88**, 236401 (2002); V. Orlyanchik and Z. Ovadyahu, *ibid.* **92**, 066801 (2004).

[54] H-D. Chen and Z. Nussinov, J. Phys. A: Math. Theor. **41**, 075001 (2008).

[55] C. Xu and J. E. Moore, Nucl. Phys. B **716**, 487 (2005); Phys. Rev. Lett. **93**, 047003 (2004).

[56] J. E. Moore and D.-H. Lee, Phys. Rev. B **69**, 104511 (2004).

[57] J. van den Brink, New J. Phys. **6**, 201 (2004).

[58] J. L. Martin, Proc. R. Soc. A **251**, 536 (1959); A. M. Tsvelik, Phys. Rev. Lett. **69**, 2142 (1992); P. Coleman, E. Miranda, and A. Tsvelik, *ibid.* **70**, 2960 (1993); B. S. Shastry and Diptiman Sen, Phys. Rev. B **55**, 2988 (1997); F. Wang and A. Vishwanath, *ibid.* **80**, 064413 (2009).

[59] Z. Nussinov and E. Fradkin, Phys. Rev. B **71**, 195120 (2005).

[60] J. Jersak, C. B. Lang, and T. Neuhas, Phys. Rev. Lett. **77**, 1933 (1996).